High-order compact schemes for parabolic problems with mixed derivatives in multiple space dimensions

Article (Published Version)

SIAM J. NUMER. ANAL.
Vol. 53, No. 5, pp. 2113–2134

HIGH-ORDER COMPACT SCHEMES FOR PARABOLIC PROBLEMS WITH MIXED DERIVATIVES IN MULTIPLE SPACE DIMENSIONS*

BERTRAM DÜRING† AND CHRISTOF HEUER‡

Abstract. We present a high-order compact finite difference approach for a class of parabolic partial differential equations with time- and space-dependent coefficients as well as with mixed second-order derivative terms in n spatial dimensions. Problems of this type arise frequently in computational fluid dynamics and computational finance. We derive general conditions on the coefficients which allow us to obtain a high-order compact scheme which is fourth-order accurate in space and second-order accurate in time. Moreover, we perform a thorough von Neumann stability analysis of the Cauchy problem in two and three spatial dimensions for vanishing mixed derivative terms, and also give partial results for the general case. The results suggest unconditional stability of the scheme. As an application example we consider the pricing of European power put basket options in the multidimensional Black–Scholes model for two and three underlying assets. Due to the low regularity of typical initial conditions we employ the smoothing operators of Kreiss, Thomee, and Widlund [*Comm. Pure Appl. Math.*, 23 (1970), pp. 241–259] to ensure high-order convergence of the approximations of the smoothed problem to the true solution.

Key words. high-order compact scheme, parabolic partial differential equation, mixed derivatives, stability

AMS subject classifications. 65M06, 65M12, 91G60

DOI. 10.1137/140974833

1. Introduction.

In the last decades, starting with the early efforts of Gupta, Manohar, and Stephenson [9, 10], high-order compact finite difference schemes have been proposed for the numerical approximation of solutions to elliptic [19, 1] and parabolic [20, 12] partial differential equations. These schemes are able to exploit the smoothness of solutions to such problems and allow one to achieve high-order numerical convergence rates (typically strictly larger than two in the spatial discretization parameter) while generally having good stability properties. Compared to finite element approaches, the high-order compact schemes are parsimonious and memory-efficient to implement and hence prove to be a viable alternative if the complexity of the computational domain is not an issue. It would be possible to achieve higher-order approximations also by increasing the computational stencil, but this leads to increased bandwidth of the discretization matrices and complicates formulations of boundary conditions. Moreover, such approaches sometimes suffer from restrictive stability conditions and spurious numerical oscillations. These problems do not arise when using a compact stencil.

Although applied successfully to many important applications, e.g., in computational fluid dynamics [18, 16, 15, 8] and computational finance [5, 6, 22, 2, 4], an even wider breakthrough of the high-order compact methodology has been hampered by

*Received by the editors June 27, 2014; accepted for publication (in revised form) June 22, 2015; published electronically September 2, 2015.
http://www.siam.org/journals/sinum/53-5/97483.html
†Department of Mathematics, University of Sussex, Pevensey II, Brighton, BN1 9QH, United Kingdom (b.during@sussex.ac.uk).
‡Lehrstuhl für Angewandte Mathematik und Numerische Analysis, Fachbereich C, Bergische Universität Wuppertal, 42119 Wuppertal, Germany (cheuer@uni-wuppertal.de). The research of this author was supported by the European Union in the FP7-PEOPLE-2012-ITN Program under Grant Agreement Number 304617 (FP7 Marie Curie Action, Project Multi-ITN *STRIKE - Novel Methods in Computational Finance*).

the algebraic complexity that is inherent to this approach. The derivation of high-order compact schemes is algebraically demanding; hence these schemes are often tailor-made for a specific application or a rather smaller class of problems (with some notable exceptions as, for example, Lele's paper [14]). The algebraic complexity is even higher in the numerical stability analysis of these schemes. Unlike for standard second-order schemes, the established stability notions imply formidable algebraic problems for high-order compact schemes. As a result, there are relatively few stability results for high-order compact schemes in the literature. This is even more pronounced in higher spatial dimension, as most of the existing studies with analytical stability results for high-order compact schemes are limited to a one-dimensional setting.

Most works focus on the isotropic case where the main part of the differential operator is given by the Laplacian. Another layer of complexity is added when the anisotropic case is considered and mixed second-order derivative terms are present in the operator. Few works on high-order compact schemes address this problem, and they study either constant coefficient problems [7] or specific equations [2].

Consequently, our aim in the present paper is to establish a high-order compact methodology for a class of parabolic partial differential equations with time- and space-dependent coefficients and mixed second-order derivative terms in arbitrary spatial dimensions. We derive general conditions on the coefficients which allow us to obtain a high-order compact scheme which is fourth-order accurate in space and second-order accurate in time. Moreover, we perform a von Neumann stability analysis of the Cauchy problem in two and three spatial dimensions for vanishing mixed derivative terms, and also give partial results for the general case. As an application example we consider the pricing of European power put basket options with two and three underlying assets in the multidimensional Black–Scholes model. The partial differential equation features second-order mixed derivative terms and, as an additional difficulty, is supplemented by an initial condition with low regularity. We use the smoothing operators of Kreiss, Thomee, and Widlund [13] to restore high-order convergence.

The rest of this paper is organized as follows. In the next section, we state the general parabolic partial differential equation in n spatial dimensions and give the central difference approximation for the associated elliptic problem. We then derive auxiliary relations for the higher-order derivatives appearing in the truncation error of the central difference approximation in section 3. In section 4 we give conditions on the coefficients of the partial differential equation under which a high-order compact scheme is obtainable. Semidiscrete high-order compact schemes in $n = 2$ and $n = 3$ space dimensions are derived in section 5. Section 6 discusses the time discretization. A thorough von Neumann stability analysis of the Cauchy problem in $n = 2$ and $n = 3$ space dimensions is performed in section 7. In section 8 we apply the schemes to option pricing problems for European power put basket options and report results of our numerical experiments in section 9. Section 10 concludes the paper.

2. Parabolic problem and its central difference approximation. We consider the following parabolic partial differential equation with mixed derivative terms in n spatial dimensions for $u = u(x_1, \dots, x_n, \tau)$:

$$u_\tau + \sum_{i=1}^{n} a_i \frac{\partial^2 u}{\partial x_i^2} + \sum_{\substack{i,j=1 \\ i<j}}^{n} b_{ij} \frac{\partial^2 u}{\partial x_i \partial x_j} + \sum_{i=1}^{n} c_i \frac{\partial u}{\partial x_i} = g \quad \text{in } \Omega \times \Omega_\tau, \tag{2.1}$$

with initial condition $u_0 = u(x_1, \dots, x_n, 0)$ and suitable boundary conditions, with space- and time-dependent coefficients $a_i = a_i(x_1, \dots, x_n, \tau) < 0, b_{ij} = b_{ij}(x_1, \dots, x_n, \tau)$, $c_i = c_i(x_1, \dots, x_n, \tau)$, and $g = g(x_1, \dots, x_n, \tau)$. The spatial domain $\Omega \subset \mathbb{R}^n$ is of n-dimensional rectangular shape with $\Omega = \Omega_1 \times \cdots \times \Omega_n$ and $x_i \in \Omega_i = \left[x_{\min}^{(i)}, x_{\max}^{(i)}\right]$ with $x_{\min}^{(i)} < x_{\max}^{(i)}$ for $i \in \{1, \dots, n\}$. The temporal domain is given by $\Omega_\tau =]0, \tau_{\max}]$ with $\tau_{\max} > 0$. The functions $a(\cdot, \tau)$, $b(\cdot, \tau)$, $c(\cdot, \tau)$, and $g(\cdot, \tau)$ are assumed to be in $C^2(\Omega)$ for any $\tau \in \Omega_\tau$, $u(\cdot, \tau) \in C^6(\Omega)$, and u is assumed to be differentiable with respect to τ. Introducing $f := -u_\tau + g$, we can rewrite (2.1) as

$$\sum_{i=1}^{n} a_i \frac{\partial^2 u}{\partial x_i^2} + \sum_{\substack{i,j=1 \\ i<j}}^{n} b_{ij} \frac{\partial^2 u}{\partial x_i \partial x_j} + \sum_{i=1}^{n} c_i \frac{\partial u}{\partial x_i} = f. \tag{2.2}$$

We start by defining a grid on Ω,

$$G^{(n)} := \left\{ \left(x_{i_1}^{(1)}, x_{i_2}^{(2)}, \dots, x_{i_n}^{(n)}\right) \in \Omega \mid x_{i_k}^{(k)} = x_{\min}^{(k)} + i_k \Delta x_k, 0 \le i_k \le N_k,\ k = 1, 2, \dots, n \right\}, \tag{2.3}$$

where $\Delta x_k = (x_{\max}^{(k)} - x_{\min}^{(k)})/N_k > 0$ are the step sizes in the kth direction with $N_k \in \mathbb{N}$ for $k = 1, 2, \dots, n$. We use $\mathring{G}^{(n)}$ for the interior of $G^{(n)}$. On this grid we denote by $U_{i_1, \dots, i_n}$ the discrete approximation of the continuous solution u at the point $\left(x_{i_1}^{(1)}, x_{i_2}^{(2)}, \dots, x_{i_n}^{(n)}\right) \in G^{(n)}$ and time $\tau \in \Omega_\tau$. Using the central difference operator D_k^c and the standard second-order central difference operator D_k^2 in the x_k-direction, we get

$$\begin{aligned}
\frac{\partial^2 u}{\partial x_k^2} &= D_k^2 u - \frac{(\Delta x_k)^2}{12} \frac{\partial^4 u}{\partial x_k^4} + \mathcal{O}\left((\Delta x_k)^4\right), \\
\frac{\partial u}{\partial x_k} &= D_k^c u - \frac{(\Delta x_k)^2}{6} \frac{\partial^3 u}{\partial x_k^3} + \mathcal{O}\left((\Delta x_k)^4\right), \\
\frac{\partial^2 u}{\partial x_k \partial x_p} &= D_k^c D_p^c u - \frac{(\Delta x_k)^2}{6} \frac{\partial^4 u}{\partial x_k^3 \partial x_p} - \frac{(\Delta x_p)^2}{6} \frac{\partial^4 u}{\partial x_k \partial x_p^3} + \mathcal{O}\left((\Delta x_k)^4\right) \\
&\quad + \mathcal{O}\left((\Delta x_k)^2 (\Delta x_p)^2\right) + \mathcal{O}\left((\Delta x_p)^4\right) + \mathcal{O}\left(\frac{(\Delta x_k)^6}{\Delta x_p}\right)
\end{aligned} \tag{2.4}$$

for $k, p \in \{1, 2, \dots, n\}$ and $k \neq p$, evaluated at the grid points $(x_{i_1}^{(1)}, x_{i_2}^{(2)}, \dots, x_{i_n}^{(n)}) \in \mathring{G}^{(n)}$. Using the approximations (2.4) in (2.2) gives

$$\begin{aligned}
f = &\sum_{i=1}^{n} a_i D_i^2 u + \sum_{\substack{i,j=1 \\ i<j}}^{n} b_{ij} D_i^c D_j^c u + \sum_{i=1}^{n} c_i D_i^c u - \sum_{i=1}^{n} \frac{a_i (\Delta x_i)^2}{12} \frac{\partial^4 u}{\partial x_i^4} \\
&- \sum_{\substack{i,j=1 \\ i<j}}^{n} b_{ij} \left[\frac{(\Delta x_i)^2}{6} \frac{\partial^4 u}{\partial x_i^3 \partial x_j} + \frac{(\Delta x_j)^2}{6} \frac{\partial^4 u}{\partial x_i \partial x_j^3} \right] - \sum_{i=1}^{n} \frac{c_i (\Delta x_i)^2}{6} \frac{\partial^3 u}{\partial x_i^3} + \varepsilon,
\end{aligned} \tag{2.5}$$

where $\varepsilon \in \mathcal{O}\left(h^4\right)$ if $\Delta x_i \in \mathcal{O}(h)$ for $i = 1, 2, \dots, n$ for a step size $h > 0$. If the consistency error is in $\mathcal{O}\left(h^4\right)$, we call the scheme high-order. In order to achieve a high-order scheme, we need to find second-order approximations of the derivatives

$\frac{\partial^3 u}{\partial x_i^3}$, $\frac{\partial^4 u}{\partial x_i^4}$, and $\frac{\partial^4 u}{\partial x_i^3 \partial x_j}$ for $i, j \in \{1, \dots, n\}$ with $i \neq j$. We call the scheme high-order compact if we can achieve this using only points from a compact computational stencil for $x = \big(x_{i_1}^{(1)}, x_{i_2}^{(2)}, \dots, x_{i_n}^{(n)}\big) \in \mathring{G}^{(n)}$. We have

(2.6)
$$\hat{U}(x) = \Big\{ \big(x_{i_1+k_1}^{(1)}, x_{i_2+k_2}^{(2)}, \dots, x_{i_n+k_n}^{(n)}\big) \in G^{(n)} \mid k_m \in \{-1, 0, 1\} \text{ for } m = 1, 2, \dots, n \Big\}$$

for $x = \big(x_{i_1}^{(1)}, x_{i_2}^{(2)} \dots, x_{i_n}^{(n)}\big)$ as the compact computational stencil and define $U_{i_1,\dots,i_n} \approx u\big(x_{i_1}^{(1)}, x_{i_2}^{(2)}, \dots, x_{i_n}^{(n)}\big)$.

3. Auxiliary relations for higher derivatives. In this section we calculate auxiliary relations for the higher derivatives appearing in (2.5). These relations for the higher derivatives can be calculated by differentiating (2.2). In doing so no additional error is introduced. Differentiating (2.2) with respect to x_k and then solving for $\frac{\partial^3 u}{\partial x_k^3}$ leads to

$$\begin{aligned}\frac{\partial^3 u}{\partial x_k^3} =& -\sum_{\substack{i=1\\ i\neq k}}^{n} \frac{a_i}{a_k} \frac{\partial^3 u}{\partial x_i^2 \partial x_k} - \sum_{\substack{i=1\\ i\neq k}}^{n} \frac{1}{a_k} \frac{\partial a_i}{\partial x_k} \frac{\partial^2 u}{\partial x_i^2} - \frac{1}{a_k} \frac{\partial a_k}{\partial x_k} \frac{\partial^2 u}{\partial x_k^2} - \sum_{\substack{i,j=1\\ i<j}}^{n} \frac{b_{ij}}{a_k} \frac{\partial^3 u}{\partial x_i \partial x_j \partial x_k} \\ & - \sum_{\substack{i,j=1\\ i<j}}^{n} \frac{1}{a_k} \frac{\partial b_{ij}}{\partial x_k} \frac{\partial^2 u}{\partial x_i \partial x_j} - \sum_{i=1}^{n} \frac{c_i}{a_k} \frac{\partial^2 u}{\partial x_i \partial x_k} - \sum_{i=1}^{n} \frac{1}{a_k} \frac{\partial c_i}{\partial x_k} \frac{\partial u}{\partial x_i} + \frac{1}{a_k} \frac{\partial f}{\partial x_k} =: A_k \end{aligned} \tag{3.1}$$

for $k = 1, \dots, n$. The relation for A_k can be approximated with consistency order two on the compact stencil (2.6) by using the central difference operator, as all derivatives of u in the above equation are only differentiated up to twice in each direction.

Differentiating (2.2) twice with respect to x_k, and solving the resulting equation for $\frac{\partial^4 u}{\partial x_k^4}$, we obtain

$$\begin{aligned}\frac{\partial^4 u}{\partial x_k^4} =& -\sum_{\substack{i=1\\ i\neq k}}^{n} \left[\frac{a_i}{a_k} \frac{\partial^4 u}{\partial x_i^2 \partial x_k^2} + \frac{2}{a_k} \frac{\partial a_i}{\partial x_k} \frac{\partial^3 u}{\partial x_i^2 \partial x_k} + \frac{1}{a_k} \frac{\partial^2 a_i}{\partial x_k^2} \frac{\partial^2 u}{\partial x_i^2} \right] - \frac{2}{a_k} \frac{\partial a_k}{\partial x_k} \frac{\partial^3 u}{\partial x_k^3} \\ & - \frac{1}{a_k} \frac{\partial^2 a_k}{\partial x_k^2} \frac{\partial^2 u}{\partial x_k^2} - \sum_{\substack{i,j=1\\ i<j\\ i,j\neq k}}^{n} \left[\frac{b_{ij}}{a_k} \frac{\partial^4 u}{\partial x_i \partial x_j \partial x_k^2} + \frac{2}{a_k} \frac{\partial b_{ij}}{\partial x_k} \frac{\partial^3 u}{\partial x_i \partial x_j \partial x_k} + \frac{1}{a_k} \frac{\partial^2 b_{ij}}{\partial x_k^2} \frac{\partial^2 u}{\partial x_i \partial x_j} \right] \\ & - \sum_{i=1}^{k-1} \frac{b_{ik}}{a_k} \frac{\partial^4 u}{\partial x_i \partial x_k^3} - \sum_{i=1}^{k-1} \left[\frac{2}{a_k} \frac{\partial b_{ik}}{\partial x_k} \frac{\partial^3 u}{\partial x_i \partial x_k^2} + \frac{1}{a_k} \frac{\partial^2 b_{ik}}{\partial x_k^2} \frac{\partial^2 u}{\partial x_i \partial x_k} \right] \\ & - \sum_{j=k+1}^{n} \frac{b_{kj}}{a_k} \frac{\partial^4 u}{\partial x_j \partial x_k^3} - \sum_{j=k+1}^{n} \left[\frac{2}{a_k} \frac{\partial b_{kj}}{\partial x_k} \frac{\partial^3 u}{\partial x_j \partial x_k^2} + \frac{1}{a_k} \frac{\partial^2 b_{kj}}{\partial x_k^2} \frac{\partial^2 u}{\partial x_j \partial x_k} \right] \\ & - \sum_{i=1}^{n} \left[\frac{c_i}{a_k} \frac{\partial^3 u}{\partial x_i \partial x_k^2} + \frac{2}{a_k} \frac{\partial c_i}{\partial x_k} \frac{\partial^2 u}{\partial x_i \partial x_k} + \frac{1}{a_k} \frac{\partial^2 c_i}{\partial x_k^2} \frac{\partial u}{\partial x_i} \right] + \frac{1}{a_k} \frac{\partial^2 f}{\partial x_k^2} \\ =:& B_k - \sum_{i=1}^{k-1} \frac{b_{ik}}{a_k} \frac{\partial^4 u}{\partial x_i \partial x_k^3} - \sum_{j=k+1}^{n} \frac{b_{kj}}{a_k} \frac{\partial^4 u}{\partial x_j \partial x_k^3}. \end{aligned} \tag{3.2}$$

We can approximate B_k with second-order consistency on the compact stencil (2.6), by using the central difference operator and the auxiliary relations for A_k in (3.1) for $k = 1, \ldots, n$. Differentiating (2.2) once with respect to x_k and once with respect to x_p leads to

$$\begin{aligned}
&a_k \frac{\partial^4 u}{\partial x_k^3 \partial x_p} + a_p \frac{\partial^4 u}{\partial x_k \partial x_p^3} \\
&= -\sum_{\substack{i=1 \\ i \neq k,p}}^{n} \left[a_i \frac{\partial^4 u}{\partial x_i^2 \partial x_k \partial x_p} + \frac{\partial a_i}{\partial x_k} \frac{\partial^3 u}{\partial x_i^2 \partial x_p} + \frac{\partial a_i}{\partial x_p} \frac{\partial^3 u}{\partial x_i^2 \partial x_k} + \frac{\partial^2 a_i}{\partial x_k \partial x_p} \frac{\partial^2 u}{\partial x_i^2} \right] - \frac{\partial a_p}{\partial x_k} \frac{\partial^3 u}{\partial x_p^3} \\
&\quad - \frac{\partial a_p}{\partial x_p} \frac{\partial^3 u}{\partial x_p^2 \partial x_k} - \frac{\partial^2 a_p}{\partial x_k \partial x_p} \frac{\partial^2 u}{\partial x_p^2} - \frac{\partial a_k}{\partial x_k} \frac{\partial^3 u}{\partial x_k^2 \partial x_p} - \frac{\partial a_k}{\partial x_p} \frac{\partial^3 u}{\partial x_k^3} - \frac{\partial^2 a_k}{\partial x_k \partial x_p} \frac{\partial^2 u}{\partial x_k^2} \\
&\quad - \sum_{\substack{i,j=1 \\ i<j}}^{n} \left[b_{ij} \frac{\partial^4 u}{\partial x_i \partial x_j \partial x_k \partial x_p} + \frac{\partial b_{ij}}{\partial x_k} \frac{\partial^3 u}{\partial x_i \partial x_j \partial x_p} + \frac{\partial b_{ij}}{\partial x_p} \frac{\partial^3 u}{\partial x_i \partial x_j \partial x_k} + \frac{\partial^2 b_{ij}}{\partial x_k \partial x_p} \frac{\partial^2 u}{\partial x_i \partial x_j} \right] \\
&\quad - \sum_{i=1}^{n} \left[c_i \frac{\partial^3 u}{\partial x_i \partial x_k \partial x_p} + \frac{\partial c_i}{\partial x_k} \frac{\partial^2 u}{\partial x_i \partial x_p} + \frac{\partial c_i}{\partial x_p} \frac{\partial^2 u}{\partial x_i \partial x_k} + \frac{\partial^2 c_i}{\partial x_k \partial x_p} \frac{\partial u}{\partial x_i} \right] + \frac{\partial^2 f}{\partial x_k \partial x_p} =: C_{kp},
\end{aligned}$$

where C_{kp} can be approximated on the compact stencil (2.6) by using A_k and A_p, as defined in (3.1), and the central difference operator for $k, p = 1, \ldots, n$ with $k \neq p$. This can be written as

$$\frac{\partial^4 u}{\partial x_k^3 \partial x_p} = \frac{C_{kp}}{a_k} - \frac{a_p}{a_k} \frac{\partial^4 u}{\partial x_k \partial x_p^3}. \tag{3.3}$$

4. Conditions for obtaining a high-order compact scheme. In this section we derive conditions on the coefficients of the partial differential equation (2.1) under which it is possible to obtain a high-order compact scheme, i.e., only using points of the n-dimensional compact stencil (2.6) for discretization and receiving a fourth-order scheme with $\Delta x_i \in \mathcal{O}(h)$ for $j = 1, \ldots, n$ for a given step size $h > 0$. Using (3.1) and (3.2) and then (3.3) in (2.5) leads to

$$\begin{aligned}
f =& \sum_{i=1}^{n} a_i D_i^2 u + \sum_{\substack{i,j=1 \\ i<j}}^{n} b_{ij} D_i^c D_j^c u + \sum_{i=1}^{n} c_i D_i^c u - \sum_{i=1}^{n} \frac{a_i (\Delta x_i)^2 B_i}{12} + \varepsilon \\
&- \sum_{\substack{i,j=1 \\ i<j}}^{n} \frac{b_{ij} (\Delta x_i)^2 C_{ij}}{12 a_i} - \sum_{\substack{i,j=1 \\ i<j}}^{n} \frac{b_{ij}}{12} \frac{\partial^4 u}{\partial x_i \partial x_j^3} \left[(\Delta x_j)^2 - \frac{a_j (\Delta x_i)^2}{a_i} \right] - \sum_{i=1}^{n} \frac{c_i (\Delta x_i)^2 A_i}{6},
\end{aligned} \tag{4.1}$$

where $\varepsilon \in \mathcal{O}\left(h^4\right)$, if $\Delta x_i \in \mathcal{O}(h)$ for $i = 1, \ldots, n$. The leading error terms are given by $\frac{b_{ij}}{12} \frac{\partial^4 u}{\partial x_i \partial x_j^3} [(\Delta x_j)^2 - \frac{a_j (\Delta x_i)^2}{a_i}]$ for $i, j \in \{1, \ldots, n\}$ with $i \neq j$. If the condition

$$b_{ij} = 0 \quad \text{or} \quad \frac{(\Delta x_j)^2}{(\Delta x_i)^2} = \frac{a_j}{a_i} \tag{4.2}$$

is fulfilled for all $i, j \in \{1, \ldots, n\}$ with $i \neq j$, these second-order terms vanish, and the resulting error term is of fourth order. Hence, for any partial differential equation

(2.1) which satisfies (4.2) we obtain a high-order compact scheme. In the case $b_{i,j} \equiv 0$ for all $i, j \in 1, \dots, n$, it is possible to choose $\Delta x_i > 0$ freely for each spatial direction, whereas in other possible cases there are interdependencies for at least some of the step sizes. For each pair (i, j) with $b_{ij} \neq 0$, the condition $\frac{(\Delta x_j)^2}{(\Delta x_i)^2} = \frac{a_j}{a_i}$ has to hold for all $x = (x_{i_1}^{(1)}, x_{i_2}^{(2)}, \dots, x_{i_n}^{(n)}) \in \mathring{G}^{(n)}$. This means a_j/a_i has to be constant as $(\Delta x_j)^2/(\Delta x_i)^2$ is constant; see (2.3).

5. Semidiscrete high-order compact schemes. In this section we present the semidiscrete high-order compact schemes in spatial dimensions $n = 2, 3$. We consider the case where the cross-derivatives do not vanish; hence we assume, for the sake of simplicity, $a_i \equiv a$ in combination with $\Delta x_i = h > 0$ for $i = 1, \dots, n$ to satisfy condition (4.2). Our aim in this section is to derive a semidiscrete scheme of the form

$$\sum_{\hat{x} \in G^{(n)}} [M_x(\hat{x}, \tau)\partial_\tau U_{i_1,\dots,i_n}(\tau) + K_x(\hat{x}, \tau)U_{i_1,\dots,i_n}(\tau)] = \tilde{g}(x, \tau) \tag{5.1}$$

at each point $x \in \mathring{G}^{(n)}$ with $\Delta x_i = h > 0$ for $i = 1, \dots, n$ and time τ, where the function $\tilde{g} : \mathring{G}^{(n)} \times \Omega_\tau \to \mathbb{R}$ depends on the function g given in (2.1).

5.1. Semidiscrete two-dimensional scheme. In this section we derive the high-order compact discretization of (2.1) in spatial dimension $n = 2$. Considering the grid point $(x_{i_1}^{(1)}, x_{i_2}^{(2)}) \in \mathring{G}^{(2)}$ with $\Delta x_1 = \Delta x_2 = h > 0$ and time $\tau \in \Omega_\tau$, we are able to obtain the coefficients $\hat{K}_{l,m}$ of $U_{l,m}(\tau)$ for $l \in \{i_1 - 1, i_1, i_1 + 1\}$ and $m \in \{i_2 - 1, i_2, i_2 + 1\}$ on the compact stencil by employing the central difference operator in (4.1). To streamline notation we denote by $[\cdot]_k$ the first derivative with respect to x_k and by $[\cdot]_{kp}$ the second derivative, once in the x_k- and once in the x_p-direction with $k, p \in \{1, 2\}$. Note that in the following the functions a, $b_{1,2}$, c_1, c_2, and g are evaluated at $(x_{i_1}^{(1)}, x_{i_2}^{(2)}) \in \mathring{G}^{(2)}$ and $\tau \in \Omega_\tau$. We omit these arguments for the sake of readability. The coefficients are given by

$$\begin{aligned}
\hat{K}_{i_1,i_2} =& -\frac{b_{12}[a]_{12}}{3a} - \frac{b_{12}[c_2]_1}{6a} + \frac{b_{12}[a]_2c_1}{6a^2} + \frac{2b_{12}[a]_1[a]_2}{3a^2} - \frac{[a]_{22}}{3} - \frac{c_1^2}{6a} + \frac{2[a]_1^2}{3a} \\
& - \frac{[a]_{11}}{3} - \frac{10a}{3h^2} - \frac{[c_2]_2}{3} - \frac{[c_1]_1}{3} - \frac{b_{12}[c_1]_2}{6a} + \frac{2[a]_2^2}{3a} - \frac{c_2^2}{6a} + \frac{b_{12}^2}{3ah^2} + \frac{b_{12}[a]_1c_2}{6a^2}, \\
\hat{K}_{i_1\pm1,i_2} =& \frac{c_2[a]_2}{12a} - \frac{b_{12}^2}{6ah^2} + \frac{b_{12}[a]_{12}}{12a} - \frac{c_1[a]_1}{12a} \mp \frac{hb_{12}[a]_2[c_1]_1}{24a^2} \mp \frac{hb_{12}[a]_1[c_1]_2}{24a^2} \pm \frac{h[c_1]_{11}}{24} \\
& \pm \frac{h[c_1]_{22}}{24} + \frac{c_1^2}{12a} \pm \frac{hc_1[c_1]_1}{24a} \mp \frac{h[a]_1[c_1]_1}{12a} \pm \frac{hb_{12}[c_1]_{12}}{24a} - \frac{b_{12}[a]_2c_1}{12a^2} \pm \frac{hc_2[c_1]_2}{24a} \\
& \mp \frac{h[a]_2[c_1]_2}{12a} + \frac{[c_1]_1}{6} - \frac{[a]_1^2}{6a} - \frac{[a]_2^2}{6a} + \frac{[a]_{22}}{12} + \frac{[a]_{11}}{12} \mp \frac{c_2b_{12}}{6ah} \mp \frac{b_{12}[b_{12}]_1}{12ah} \\
& + \frac{b_{12}[c_1]_2}{12a} + \frac{2a}{3h^2} - \frac{b_{12}[a]_1[a]_2}{6a^2} \pm \frac{b_{12}[a]_2}{6ah} \mp \frac{[b_{12}]_2}{6h} \pm \frac{b_{12}^2[a]_1}{12a^2h} \pm \frac{c_1}{3h}, \\
\hat{K}_{i_1,i_2\pm1} =& -\frac{c_2[a]_2}{12a} - \frac{b_{12}^2}{6ah^2} + \frac{b_{12}[c_2]_1}{12a} + \frac{b_{12}[a]_{12}}{12a} + \frac{c_1[a]_1}{12a} \mp \frac{hb_{12}[a]_2[c_2]_1}{24a^2} + \frac{[c_2]_2}{6} \\
& \mp \frac{hb_{12}[a]_1[c_2]_2}{24a^2} - \frac{[a]_1^2}{6a} - \frac{[a]_2^2}{6a} + \frac{c_2^2}{12a} + \frac{[a]_{22}}{12} + \frac{[a]_{11}}{12} \mp \frac{b_{12}[b_{12}]_2}{12ah} \pm \frac{h[c_2]_{22}}{24} \\
& \pm \frac{h[c_2]_{11}}{24} + \frac{2a}{3h^2} \pm \frac{hc_1[c_2]_1}{24a} \mp \frac{h[a]_1[c_2]_1}{12a} - \frac{b_{12}[a]_1[a]_2}{6a^2} \pm \frac{hb_{12}[c_2]_{12}}{24a} \pm \frac{c_2}{3h} \\
& - \frac{b_{12}[a]_1c_2}{12a^2} \mp \frac{h[a]_2[c_2]_2}{12a} \pm \frac{hc_2[c_2]_2}{24a} \pm \frac{b_{12}^2[a]_2}{12a^2h} \pm \frac{b_{12}[a]_1}{6ah} \mp \frac{c_1b_{12}}{6ah} \mp \frac{[b_{12}]_1}{6h},
\end{aligned}$$

$$
\begin{aligned}
\hat{K}_{i_1\pm1,i_2-1} = {} & \frac{b_{12}^2}{12ah^2} \mp \frac{c_1c_2}{24a} \pm \frac{[a]_2c_1}{24a} \mp \frac{b_{12}[c_2]_2}{48a} \pm \frac{[a]_2[b_{12}]_2}{24a} \pm \frac{[a]_1c_2}{24a} \pm \frac{[a]_1[b_{12}]_1}{24a} \\
& \mp \frac{c_1[b_{12}]_1}{48a} \mp \frac{b_{12}[c_1]_1}{48a} \mp \frac{c_2[b_{12}]_2}{48a} \mp \frac{b_{12}[b_{12}]_{12}}{48a} \mp \frac{[c_1]_2}{24} \mp \frac{[c_2]_1}{24} \mp \frac{[b_{12}]_{11}}{48} \\
& \mp \frac{[b_{12}]_{22}}{48} \mp \frac{b_{12}[b_{12}]_2}{24ah} \pm \frac{c_2b_{12}}{12ah} \pm \frac{b_{12}[b_{12}]_1}{24ah} \pm \frac{b_{12}[a]_2[b_{12}]_1}{48a^2} \pm \frac{b_{12}[a]_1c_1}{48a^2} + \frac{a}{6h^2} \\
& + \frac{b_{12}^2[a]_2}{24a^2h} \pm \frac{b_{12}[a]_2c_2}{48a^2} + \frac{b_{12}[a]_1}{12ah} \mp \frac{b_{12}[a]_2}{12ah} - \frac{c_1b_{12}}{12ah} \pm \frac{b_{12}[a]_1[b_{12}]_2}{48a^2} - \frac{[b_{12}]_1}{12h} \\
& \pm \frac{[b_{12}]_2}{12h} \mp \frac{b_{12}^2[a]_1}{24a^2h} \mp \frac{b_{12}}{4h^2} - \frac{c_2}{12h} \pm \frac{c_1}{12h}, \\
\hat{K}_{i_1\pm1,i_2+1} = {} & \frac{b_{12}^2}{12ah^2} \pm \frac{c_1c_2}{24a} \mp \frac{[a]_2c_1}{24a} \pm \frac{b_{12}[c_2]_2}{48a} \mp \frac{[a]_2[b_{12}]_2}{24a} \mp \frac{[a]_1c_2}{24a} \mp \frac{[a]_1[b_{12}]_1}{24a} \\
& \pm \frac{c_1[b_{12}]_1}{48a} \pm \frac{b_{12}[c_1]_1}{48a} \pm \frac{c_2[b_{12}]_2}{48a} \pm \frac{b_{12}[b_{12}]_{12}}{48a} \pm \frac{[c_1]_2}{24} \pm \frac{[c_2]_1}{24} \pm \frac{[b_{12}]_{11}}{48} \\
& \pm \frac{[b_{12}]_{22}}{48} + \frac{b_{12}[b_{12}]_2}{24ah} \pm \frac{c_2b_{12}}{12ah} \pm \frac{b_{12}[b_{12}]_1}{24ah} \mp \frac{b_{12}[a]_2[b_{12}]_1}{48a^2} \mp \frac{b_{12}[a]_1c_1}{48a^2} + \frac{a}{6h^2} \\
& - \frac{b_{12}^2[a]_2}{24a^2h} \mp \frac{b_{12}[a]_2c_2}{48a^2} - \frac{b_{12}[a]_1}{12ah} \mp \frac{b_{12}[a]_2}{12ah} + \frac{c_1b_{12}}{12ah} \mp \frac{b_{12}[a]_1[b_{12}]_2}{48a^2} + \frac{[b_{12}]_1}{12h} \\
& \pm \frac{[b_{12}]_2}{12h} \mp \frac{b_{12}^2[a]_1}{24a^2h} \pm \frac{b_{12}}{4h^2} + \frac{c_2}{12h} \pm \frac{c_1}{12h}.
\end{aligned}
$$

Analogously, we obtain the coefficients $\hat{M}_{l,m}$ of $\partial_\tau U_{l,m}(\tau)$ for $l \in \{i_1-1, i_1, i_1+1\}$ and $m \in \{i_2-1, i_2, i_2+1\}$ at each point $(x_{i_1}^{(1)}, x_{i_2}^{(2)}) \in \mathring{G}^{(2)}$ and time $\tau \in \Omega_\tau$:

$$
\begin{aligned}
\hat{M}_{i_1+1,i_2\pm1} = \hat{M}_{i_1-1,i_2\mp1} = \pm\frac{b_{12}}{48a}, \quad \hat{M}_{i_1,i_2\pm1} = \frac{1}{12} \mp \frac{h[a]_2}{12a} \mp \frac{b_{12}h[a]_1}{24a^2} \pm \frac{c_2h}{24a}, \\
\hat{M}_{i_1\pm1,i_2} = \frac{1}{12} \mp \frac{b_{12}h[a]_2}{24a^2} \pm \frac{hc_1}{24a} \mp \frac{h[a]_1}{12a}, \quad \hat{M}_{i_1,i_2} = \frac{2}{3},
\end{aligned}
$$

where $\Delta x_1 = \Delta x_2 = h > 0$. Additionally, for $x \in \mathring{G}^{(2)}$, $\tau \in \Omega_\tau$,

$$
\begin{aligned}
\tilde{g}(x,\tau) = {} & \frac{\left(h^2a^2c_1 - 2h^2a^2[a]_1 - b_{12}h^2[a]_2a\right)[g]_1}{12a^3} + \frac{h^2[g]_{11}}{12} + \frac{b_{12}h^2[g]_{12}}{12a} \\
& + \frac{\left(h^2a^2c_2 - b_{12}h^2[a]_1a - 2h^2a^2[a]_2\right)[g]_{x_2}}{12a^3} + \frac{h^2[g]_{22}}{12} + g
\end{aligned}
$$

holds, where $\Delta x_1 = \Delta x_2 = h > 0$ was used. We have $K_x(x_{n_1}^{(1)}, x_{n_2}^{(2)}, \tau) = \hat{K}_{n_1,n_2}$ and $M_x(x_{n_1}^{(1)}, x_{n_2}^{(2)}, \tau) = \hat{M}_{n_1,n_2}$ in (5.1) with $n_1 \in \{i_1-1, i_1, i_1+1\}$ and $n_2 \in \{i_2-1, i_2, i_2+1\}$ for $x = (x_{i_1}^{(1)}, x_{i_2}^{(2)}) \in \mathring{G}^{(2)}$ and $\tau \in \Omega_\tau$. K_x and M_x are zero otherwise, and the approximation only uses points of the compact stencil.

5.2. Semidiscrete three-dimensional scheme. In this section we derive the high-order compact discretization of (2.1) in spatial dimension $n = 3$. Considering the conditions in (4.2), we observe that in the three-dimensional case we have three different possibilities to satisfy the conditions and thus obtain a high-order compact scheme. We focus on the case $a = a_1 \equiv a_2 \equiv a_3$ and set $h = \Delta x_1 = \Delta x_2 = \Delta x_3$. Considering an interior grid point $(x_{i_1}^{(1)}, x_{i_2}^{(2)}, x_{i_3}^{(3)}) \in \mathring{G}^{(3)}$ and time $\tau \in \Omega_\tau$, we are able to produce the coefficients $\hat{K}_{k,l,m}$ of $U_{k,l,m}(\tau)$ for $k \in \{i_1-1, i_1, i_1+1\}$, $l \in \{i_2-1, i_2, i_2+1\}$, and $m \in \{i_3-1, i_3, i_3+1\}$ by employing the central difference operator in (4.1). Again, to streamline the notation we denote by $[\cdot]_k$ and $[\cdot]_{kp}$ the

first and second derivatives of the coefficients with respect to x_k, and with respect to x_k and x_p, respectively. Note again that in the following $a, b_{12}, b_{13}, b_{23}, c_1, c_2, c_3$, and g are evaluated at $(x_{i_1}^{(1)}, x_{i_2}^{(2)}, x_{i_3}^{(3)}) \in \mathring{G}^{(3)}$ and $\tau \in \Omega_\tau$, where $\Delta x_i = h > 0$ for $i = 1, 2, 3$. We omit these arguments for the sake of readability. Due to the length of the coefficient expressions $\hat{K}_{k,l,m}$, they are given in the supplementary material accessible at the online version of this paper.

In a similar way we define $\hat{M}_{k,l,m}$ as the coefficient of $\partial_\tau U_{k,l,m}(\tau)$ for $k \in \{i_1 - 1, i_1, i_1 + 1\}$, $l \in \{i_2 - 1, i_2, i_2 + 1\}$, and $m \in \{i_3 - 1, i_3, i_3 + 1\}$ by

$$
\begin{aligned}
\hat{M}_{i_1\pm1,i_2-1,i_3} &= \hat{M}_{i_1\mp1,i_2+1,i_3} = \mp\frac{b_{12}}{48a}, \quad \hat{M}_{i_1,i_2,i_3} = \frac{1}{2},\\
\hat{M}_{i_1\pm1,i_2,i_3-1} &= \hat{M}_{i_1\mp1,i_2,i_3+1} = \mp\frac{b_{13}}{48a}, \quad \hat{M}_{i_1,i_2\pm1,i_3-1} = \hat{M}_{i_1,i_2\mp1,i_3+1} = \mp\frac{b_{23}}{48a},\\
\hat{M}_{i_1\pm1,i_2,i_3} &= \frac{1}{12} \mp \frac{hb_{12}[a]_2}{24a^2} \mp \frac{hb_{13}[a]_3}{24a^2} \pm \frac{hc_1}{24a} \mp \frac{h[a]_1}{12a},\\
\hat{M}_{i_1,i_2\pm1,i_3} &= \frac{1}{12} \mp \frac{hb_{12}[a]_1}{24a^2} \mp \frac{hb_{23}[a]_3}{24a^2} \pm \frac{hc_2}{24a} \mp \frac{h[a]_2}{12a},\\
\hat{M}_{i_1,i_2,i_3\pm1} &= \frac{1}{12} \mp \frac{hb_{23}[a]_2}{24a^2} \mp \frac{hb_{13}[a]_1}{24a^2} \pm \frac{hc_3}{24a} \mp \frac{h[a]_3}{12a},\\
\hat{M}_{i_1\pm1,i_2-1,i_3-1} &= \hat{M}_{i_1\pm1,i_2+1,i_3-1} = \hat{M}_{i_1\pm1,i_2-1,i_3+1} = \hat{M}_{i_1\pm1,i_2+1,i_3+1} = 0.
\end{aligned}
$$

For the right-hand side of (5.1) we have for $x = (x_{i_1}^{(1)}, x_{i_2}^{(2)}, x_{i_3}^{(3)}) \in \mathring{G}^{(3)}$, $\tau \in \Omega_\tau$,

$$
\begin{aligned}
\tilde{g}(x,\tau) = {} & \frac{\left(c_1h^2a - 2h^2[a]_1a - b_{12}h^2[a]_2 - b_{13}h^2[a]_3\right)[g]_1}{12a^2} + \frac{b_{13}h^2[g]_{13}}{12a}\\
& + \frac{\left(c_2h^2a - 2h^2[a]_2a - b_{12}h^2[a]_1 - b_{23}h^2[a]_3\right)[g]_2}{12a^2} + \frac{b_{23}h^2[g]_{23}}{12a}\\
& + \frac{\left(c_3h^2a - 2h^2[a]_3a - b_{13}h^2[a]_1 - b_{23}h^2[a]_2\right)[g]_3}{12a^2} + \frac{h^2[g]_{11}}{12}\\
& + \frac{b_{12}h^2[g]_{12}}{12a} + \frac{h^2[g]_{33}}{12} + \frac{h^2[g]_{22}}{12} + g.
\end{aligned}
$$

We define $K_x(x_{n_1}^{(1)}, x_{n_2}^{(2)}, x_{n_3}^{(3)}, \tau) = \hat{K}_{n_1,n_2,n_3}$ and $M_x(x_{n_1}^{(1)}, x_{n_2}^{(2)}, x_{n_3}^{(3)}, \tau) = \hat{M}_{n_1,n_2,n_3}$ for each point $x = (x_{i_1}^{(1)}, x_{i_2}^{(2)}, x_{i_3}^{(3)}) \in \mathring{G}^{(3)}$ and $\tau \in \Omega_\tau$, where $n_j \in \{i_j - 1, i_j, i_j + 1\}$ with $j = 1, 2, 3$. K_x and M_x are zero otherwise. Hence, the approximation only uses points of the compact stencil (2.6).

6. Fully discrete scheme. The semidiscrete scheme presented in the previous sections can be extended to a fully discrete scheme for the parabolic problem (2.1) by additionally discretizing in time. Any time integrator can be implemented to solve the problem as in [20]. Here we consider a Crank–Nicolson-type time discretization with constant time step $\Delta\tau$ to obtain a fully discrete scheme. Let

$$
A_x(\hat{x}, \tau_{k+1}) = \hat{M}_x(\hat{x}, \tau_k) + \frac{\Delta\tau}{2} K_x(\hat{x}, \tau_{k+1}), \; B_x(\hat{x}, \tau_k) = \hat{M}_x(\hat{x}, \tau_k) - \frac{\Delta\tau}{2} K_x(\hat{x}, \tau_k),
$$

where $\hat{M}_x(\hat{x}, \tau_k) = \left(M_x(\hat{x}, \tau_k) + M_x(\hat{x}, \tau_{k+1})\right)/2$. $K_x(\hat{x}, \tau)$ and $M_x(\hat{x}, \tau)$ are defined through a semidiscrete finite difference scheme with fourth-order consistency using only points of the compact stencil (2.6). Then, a fully discrete high-order compact

finite difference scheme for (2.1) with $n \in \mathbb{N}$ on the time grid $\tau_k = k\Delta_\tau$ for $k = 0, \ldots, N_\tau$ and $\Delta x_i = h$ for all i is given at each point $x = (x_{i_1}^{(1)}, \ldots, x_{i_n}^{(n)}) \in \overset{\circ}{G}{}^{(n)}$ by

$$\sum_{\hat{x} \in \hat{U}(x)} A_x(\hat{x}, \tau_{k+1}) U_{l_1,\ldots,l_n}^{k+1} = \sum_{\hat{x} \in \hat{U}(x)} B_x(\hat{x}, \tau_k) U_{l_1,\ldots,l_n}^{k} + \frac{\Delta\tau}{2} \hat{g}(x, \tau_k, \tau_{k+1}), \tag{6.1}$$

where $\hat{g}(x, \tau_k, \tau_{k+1}) = \tilde{g}(x, \tau_k) + \tilde{g}(x, \tau_{k+1})$ and $\hat{x} = \left(x_{l_1}^{(1)}, \ldots, x_{l_n}^{(n)}\right) \in \hat{U}(x)$. This scheme is second-order consistent in time and fourth-order consistent in space. We have fourth-order consistency in terms of h for $\Delta\tau \in \mathcal{O}(h^2)$ while only using the compact stencil. Note that up to this point only the spatial interior is discussed. The applied boundary conditions may still have an effect on the above numerical scheme.

7. Stability analysis for the Cauchy problem in dimensions $n = 2, 3$. In this section we consider the stability analysis of the high-order compact scheme for the Cauchy problem associated with (2.1) in the case $n = 2, 3$. The coefficients of the semidiscrete scheme are given in section 5.1 for two spatial dimensions, and in section 5.2 for three spatial dimensions. These coefficients are nonconstant, as the coefficients of the parabolic partial differential equation (2.1) are nonconstant.

We consider a von Neumann stability analysis. Other approaches which take into account boundary conditions, such as normal mode analysis [11], are beyond the scope of the present paper. For both $n = 2$ and $n = 3$, we give a proof of stability in the case of vanishing cross-derivative terms and frozen coefficients in time and space, which means that all possible values for the coefficients are considered, but as constants; hence the derivatives of the coefficients of the partial differential equation appearing in the discrete schemes are set to zero. This approach has also been used in [11, 21] and gives a necessary stability condition, whereas slightly stronger conditions are sufficient to ensure overall stability [17]. This approach is used extensively in the literature and yields good criteria on the robustness of the scheme. In (6.1) we use

$$U_{j_1,\ldots,j_n}^k = g^k e^{IS_n} \quad \text{with} \quad S_n = \sum_{m=1}^{n} j_m z_m$$

for $j_m \in \{i_m - 1, i_m, i_m + 1\}$, where I is the imaginary unit, g^k is the amplitude at time level k, and $z_m = 2\pi h/\lambda_m$ for the wavelength $\lambda_m \in [0, 2\pi[$ for $m = 1, \ldots, n$. Then the fully discrete scheme satisfies the *necessary von Neumann stability condition* for all z_1, z_2, when the amplification factor $G = g^{k+1}/g^k$ satisfies

$$|G|^2 - 1 \leq 0. \tag{7.1}$$

7.1. Stability analysis for the two-dimensional case. In this section we perform the von Neumann stability analysis for the two-dimensional high-order compact scheme of section 5.1. The analysis of the case with vanishing cross-derivative and frozen coefficients are carried out in detail. In the case of nonvanishing mixed derivatives partial results are given for frozen coefficients.

THEOREM 7.1. *For $a = a_1 = a_2 < 0$, $b_{1,2} = 0$, and $\Delta x_1 = \Delta x_2 = h > 0$, the fully discrete high-order compact finite difference scheme given in* (6.1) *with $n = 2$, with coefficients defined in section* 5.1*, satisfies (for frozen coefficients) the necessary stability condition* (7.1)*.*

Proof. Let $\xi_1 = \cos(z_1/2)$, $\xi_2 = \cos(z_2/2)$, $\eta_1 = \sin(z_1/2)$, and $\eta_2 = \sin(z_2/2)$. The stability condition (7.1) for the fully discrete scheme (6.1) using the coefficients

defined in section 5.1 yields $|G|^2 - 1 = N_G/D_G$ (explicit expressions for N_G, D_G are given below). We discuss the numerator N_G and the denominator D_G separately in the following.

The numerator can be written as $N_G = 8ka\left(n_4 h^4 + n_2 h^2\right)$, where the polynomials

$$n_2 = 8a^2 f_1(\xi_1,\xi_2) f_2(\xi_1,\xi_2) \quad \text{and} \quad n_4 = f_3(\xi_1) f_4(\xi_1,\xi_2) c_1^2 + f_3(\xi_2) f_4(\xi_2,\xi_1) c_2^2$$

are nonnegative, since

$$f_1(x,y) = x^2 + y^2 + 1 \geq 0, \qquad f_2(x,y) = 2 - x\Big(y^2 + \frac{1}{2}\Big) - \frac{y^2}{2} \geq 0,$$
$$f_3(x) = x^2 - 1 \leq 0, \qquad f_4(x,y) = 2x^2y^2 - x^2 - 1 \leq 0$$

for $x, y \in [-1,1]$. Hence, we observe that $N_G \leq 0$ holds, as $\xi_1, \xi_2 \in [-1,1]$.

Now we consider the denominator D_G, which can be written as

$$D_G = d_6 h^6 + \left(d_{4,2}k^2 + d_{4,1}k + d_{4,0}\right) h^4 + (d_{2,2}k^2 + d_{2,1}k)h^2 + d_0,$$

where

$$d_0 = 16a^4k^2\left(2\xi_1^2\xi_2^2 + \xi_1^2 + \xi_2^2 - 4\right)^2 \geq 0, \quad d_{2,1} = 16a^3 f_1(\xi_1,\xi_2) f_5(\xi_1,\xi_2) \geq 0,$$
$$d_{2,2} = 4a^2\left[9\left(\xi_1\eta_1 c_1 + \xi_2\eta_2 c_2\right)^2 + 2f_3(\xi_1) f_6(\xi_1,\xi_2) c_1^2 + 2f_3(\xi_2) f_6(\xi_2,\xi_1) c_2^2\right],$$
$$d_{4,0} = 4a^2 f_1(\xi_1,\xi_2)^2 \geq 0, \quad d_{4,1} = -4an_4 \geq 0,$$
$$d_{4,2} = \left[f_3(\xi_1)c_1^2 - 2\eta_1\eta_2\xi_1\xi_2 c_1 c_2 + f_3(\xi_2)c_2^2\right]^2 \geq 0, \quad d_6 = \left(\xi_1\eta_1 c_1 + \xi_2\eta_2 c_2\right)^2 \geq 0,$$

because $a < 0$ and where

$$f_5(x,y) = 2x^2y^2 + x^2 + y^2 - 4 \leq 0, \quad f_6(x,y) = 2x^2y^4 - 5x^2 - y^2 + 4$$

with $x, y \in [-1,1]$. We observe that $f_6(x,y)$ changes sign, as, for example, $f_6(0,0) = 4$ and $f_6(1,0) = -1$. Hence, we cannot determine the sign of $d_{2,2}$ directly.

If $c_1 = c_2 = 0$, we have $d_{2,2} = 0$ and hence $D_G \geq 0$. Since $d_{2,2}$ is symmetric, we can say without loss of generality that $c_1 \neq 0$ in the following. Furthermore, as both c_1 and c_2 are frozen coefficients, we set $m = c_2/c_1$, which leads to

$$d_{2,2} = 4a^2c_1^2[9(\xi_1\eta_1 + \xi_2\eta_2 m)^2 + 2f_3(\xi_1)f_6(\xi_1,\xi_2) + 2f_3(\xi_2)f_6(\xi_2,\xi_1)m^2] =: 4a^2c_1^2 g(m).$$

The function $g(m)$ can be rewritten as

$$g(m) = \eta_1^2 f_7(\xi_1,\xi_2) m^2 + 18\xi_1\xi_2\eta_1\eta_2 m + \eta_2^2 f_7(\xi_2,\xi_1)$$

with $f_7(x,y) = 4x^4y^2 - 2x^2 - y^2 + 8 \geq -2x^2 - y^2 + 8 \geq 5$. In the case $\eta_1 = 0$ we have $g(m) = \eta_2^2 f_7(\xi_2,\xi_1) \geq 0$ and thus $d_{2,2} \geq 0$ and $D_G \geq 0$. In the case $\eta_1 \neq 0$ we have $\eta_1^2 f_7(\xi_1,\xi_2) > 0$; hence the function $g(m)$ has a global minimum. This minimum is located at

$$\hat{m} = \frac{-9\xi_1\xi_2\eta_2}{\eta_1 f_7(\xi_1,\xi_2)}, \quad \text{which leads to} \quad g(\hat{m}) = \frac{2\eta_1^2 f_5(\xi_1,\xi_2) f_8}{f_7(\xi_1,\xi_2)},$$

where $f_8 = 6\xi_1^2\xi_2^2 + \xi_1^2 + \xi_2^2 - 2\xi_1^4\xi_2^2\eta_2^2 - 2\xi_1^2\eta_1^2\xi_2^4 - 8 \leq 0$. Since $f_5(\xi_1,\xi_2) \leq 0$, we have $g(m) \geq 0$ for all $m \in \mathbb{R}$, and thus we have $D_G \geq 0$ for all cases as $a < 0$.

We still need to show that $D_G > 0$ for all $\xi_1, \xi_2 \in [-1,1]$. It holds that $d_0 > 0$ for all $(\xi_1, \xi_2) \in [-1,1]^2 \setminus \{-1,1\}^2$ as $a < 0$ and $k > 0$. This leads to $D_G > 0$ in these cases. For the case $(\xi_1, \xi_2) \in \{-1,1\}^2$ it holds that $f_1(\xi_1, \xi_2) = 3$, which leads to $d_{4,0} = 36a^2 > 0$ and $D_G > 0$. Therefore, we have $D_G > 0$ for all $(\xi_1, \xi_2) \in [-1,1]^2$, and condition (7.1) is satisfied. ∎

For $b_{1,2} \neq 0$ the situation becomes much more involved. Many additional terms appear in the expression for the amplification factor G, and we face an additional degree of freedom through $b_{1,2}$. Since we have proved that condition (7.1) holds for $b_{1,2} = 0$, it seems reasonable to assume that it also holds at least for values of $b_{1,2}$ close to zero. In von Neumann stability analysis it is often most difficult to guarantee that stability condition (7.1) holds for extreme values of η_1, η_2, ξ_1, and ξ_2. We have the following partial result which holds in the case of frozen coefficients and nonvanishing coefficients of the mixed derivative, i.e., $b_{1,2} \neq 0$.

LEMMA 7.2. *For $a = a_1 = a_2 < 0$, arbitrary $b_{1,2}$, and $\Delta x_1 = \Delta x_2 = h > 0$, the high-order compact scheme* (6.1) *with the coefficients for the two-dimensional case defined in section* 5.1 *satisfies (for frozen coefficients) the stability condition* (7.1) *at the corner points $\xi_1 = \pm 1$ and $\xi_2 = \pm 1$.*

Proof. Using $\eta_1 = \sin(z_1/2) = \sqrt{1-\xi_1^2} = 0$ for $\xi_1 = \pm 1$ and $\eta_2 = \sin(z_2/2) = \sqrt{1-\xi_2^2} = 0$ for $\xi_2 = \pm 1$, straightforward computation shows that on each corner point $|G|^2 - 1 = 0$. Hence, condition (7.1) holds. ∎

It is worth mentioning that in a comparable situation in [3] (where a specific partial differential equation of type (2.1) is considered) an additional numerical evaluation of condition (7.1) revealed it to hold also for nonvanishing mixed derivatives with $(\xi_1^2, \xi_2^2) \neq (1,1)$. However, the left-hand side of (7.1) was very close to zero, and although the inequality was always satisfied, this left little room for analytical estimates. This leads to the conjecture that the stability condition in that case was satisfied also for general parameters, although it would be hard to prove analytically. Lemma 7.2 above suggests that the present case is similar. We remark that in our numerical experiments we observe a stable behavior throughout, also for a general choice of parameters.

7.2. Stability analysis for the three-dimensional case. In this section we analyze the stability of the high-order compact scheme with coefficients given in section 5.2 in three space dimensions. We first perform a thorough von Neumann stability analysis in the case of vanishing cross-derivative terms for frozen coefficients. We observe no additional stability condition in this case. Then we give partial results in the case of nonvanishing cross-derivative terms for frozen coefficients.

THEOREM 7.3. *For $a_i = a < 0$, $b_{i,j} = 0$, and $\Delta x_i = h > 0$ for $i, j \in \{1,2,3\}$, $i \neq j$, the fully discrete high-order compact scheme given in* (6.1) *with $n = 3$, with coefficients given in section* 5.2*, satisfies (for frozen coefficients) the necessary stability condition* (7.1)*.*

Proof. Let $\xi_i = \cos(z_i/2)$ and $\eta_i = \sin(z_i/2)$ for $i = 1,2,3$. The stability condition (7.1) yields $|G|^2 - 1 = N_G/D_G$ (explicit expressions for N_G, D_G are given below).

For the numerator we have $N_G = -8ak\left(n_4 h^4 + n_2 h^2\right) \leq 0$ since $a < 0$, and the polynomials

$$n_2 = 4a^2 f_1(\xi_1,\xi_2,\xi_3)\left[f_2(\xi_1,\xi_2) + f_2(\xi_3,\xi_1) + f_2(\xi_2,\xi_3)\right] \leq 0,$$

$$n_4 = \left[f_3(\xi_1,\xi_2) + f_3(\xi_1,\xi_3)\right]c_1^2 + \left[f_3(\xi_2,\xi_1) + f_3(\xi_2,\xi_3)\right]c_2^2 + \left[f_3(\xi_3,\xi_1) + f_3(\xi_3,\xi_2)\right]c_3^2$$
$$- \eta_3^2\left(\xi_1\eta_1 c_1 + \xi_2\eta_2 c_2\right)^2 - \eta_2^2\left(\xi_1\eta_1 c_1 + \xi_3\eta_3 c_3\right)^2 - \eta_1^2\left(\xi_2\eta_2 c_2 + \xi_3\eta_3 c_3\right)^2 \leq 0$$

are nonnegative since

$$f_1(x,y) = x^2+y^2+z^2 \geq 0, \qquad f_2(x,y) = 2x^2y^2 - x^2 - 1 \leq 0,$$
$$f_3(x,y) = x^2y^2\left(1-x^2\right) + y^2\left(x^2-1\right) \leq y^2\left(1-x^2\right) + y^2\left(x^2-1\right) = 0$$

for $x,y,z \in [-1,1]$.

The denominator D_G can be written as

$$D_G = d_6h^6 + \left(d_{4,2}k^2 + d_{4,1}k + d_{4,0}\right)h^4 + \left(d_{2,2}k^2 + d_{2,1}k\right)h^2 + d_0,$$

where

$$\begin{aligned}
d_0 &= 16a^4k^2\left[m_1(\xi_1,\xi_2) + m_1(\xi_3,\xi_1) + m_1(\xi_2,\xi_3)\right]^2 \geq 0, \quad d_{2,1} = 4an_2 \geq 0,\\
d_{2,2} &= 4a^2\left[m_6(\xi_1,\eta_1,\xi_2)c_1^2 + 2m_7(\xi_3)\xi_1\xi_2\eta_1\eta_2c_1c_2 + m_6(\xi_2,\eta_2,\xi_1)c_2^2\right.\\
&\quad + m_6(\xi_1,\eta_1,\xi_3)c_1^2 + 2m_7(\xi_2)\xi_1\xi_3\eta_1\eta_3c_1c_3 + m_6(\xi_3,\eta_3,\xi_1)c_3^2\\
&\quad + m_6(\xi_2,\eta_2,\xi_3)c_2^2 + 2m_7(\xi_1)\xi_2\xi_3\eta_2\eta_3c_2c_3 + m_6(\xi_3,\eta_3,\xi_2)c_3^2\\
&\quad \left. + m_5(\eta_1,\xi_2,\xi_3)c_1^2 + m_5(\eta_2,\xi_1,\xi_3)c_2^2 + m_5(\eta_3,\xi_1,\xi_2)c_3^2\right],\\
d_{4,0} &= 4a^2m_2(\xi_1,\xi_2,\xi_3)^2 \geq 0,\ d_{4,1} = 4an_4 \geq 0,\ d_6 = \left[\xi_1\eta_1c_1 + \xi_2\eta_2c_2 + \xi_3\eta_3c_3\right]^2 \geq 0,\\
d_{4,2} &= \left[\eta_1^2c_1^2 + \eta_2^2c_2^2 + \eta_3^2c_3^2 + 2\xi_1\eta_1\xi_2\eta_2c_1c_2 + 2\xi_1\eta_1\xi_3\eta_3c_1c_3 + 2\xi_2\eta_2\xi_3\eta_3c_2c_3\right]^2 \geq 0,
\end{aligned}$$

since $a < 0$ and

$$\begin{aligned}
m_1(x,y) &= 2x^2y^2 - x^2 - 1 \leq x^2 - 1 \leq 0, \quad m_2(x,y,z) = x^2+y^2+z^2 \geq 0,\\
m_3(x,y) &= x^2y^2\left(1-x^2\right) + y^2\left(x^2-1\right) \leq y^2\left(1-x^2\right) + y^2\left(x^2-1\right) = 0,\\
m_4(x,y) &= (1-x^2)[x^2(y^2-1) + y^2(x^2-1)] \leq 0,\\
m_5(x,y,z) &= -8x^4y^2z^2 + 4x^2y^2z^2 + 4x^2 \geq -8x^2y^2z^2 + 4x^2y^2z^2 + 4x^2\\
&= -4x^2y^2z^2 + 4x^2 \geq -4x^2 + 4x^2 = 0,\\
m_6(x_1,x_2,y) &= 4x_2^2x_1^2y^4 + (-8x_2^2x_1^2 + 2x_2^2)y^2 + x_2^2 + \frac{3}{2}x_1^2x_2^2 \in [0,3],\\
m_7(x) &= 2x^2(x^2 - (1-x^2)) + 7 \geq 0
\end{aligned}$$

for $x,y,z \in [-1,1]$. We still need to show $d_{2,2} \geq 0$. Since we cannot determine the sign of $d_{2,2}$ directly, we consider three different cases.

First, having $\xi_2^2 = \xi_3^2 = 1$ leads to

$$d_{2,2} = 4a^2\left[2\left(-2.5\xi_1^2\eta_1^2 + 3\eta_1^2\right)c_1^2 + \left(-8\eta_1^4 + 8\eta_1^2\right)c_1^2\right] \geq 0$$

as $\xi_1^2 \leq 1$ and $\eta_1^2 \leq 1$.

Second, we consider $c_1 = c_2 = c_3 = 0$. This leads directly to $d_{2,2} = 0$.

Third, from now on we have $(c_1,c_2,c_3) \neq (0,0,0)$. Since $d_{2,2}$ is symmetric with respect to c_1,c_2,c_3, we assume without loss of generality that $c_1 \neq 0$. Additionally, we have $\left(\xi_2^2,\xi_3^2\right) \neq (1,1)$. Setting $p_2 := c_2/c_1$ and $p_3 := c_3/c_1$ gives

$$\begin{aligned}
d_{2,2} &= 4a^2c_1^2\left[m_6(\xi_1,\eta_1,\xi_2) + 2m_7(\xi_3)\xi_1\xi_2\eta_1\eta_2p_2 + m_6(\xi_2,\eta_2,\xi_1)p_2^2\right.\\
&\quad + m_6(\xi_1,\eta_1,\xi_3) + 2m_7(\xi_2)\xi_1\xi_3\eta_1\eta_3p_3 + m_6(\xi_3,\eta_3,\xi_1)p_3^2\\
&\quad + m_6(\xi_2,\eta_2,\xi_3)p_2^2 + 2m_7(\xi_1)\xi_2\xi_3\eta_2\eta_3p_2p_3 + m_6(\xi_3,\eta_3,\xi_2)p_3^2\\
&\quad \left. + m_5(\eta_1,\xi_2,\xi_3) + m_5(\eta_2,\xi_1,\xi_3)p_2^2 + m_5(\eta_3,\xi_1,\xi_2)p_3^2\right]\\
&=: 4a^2c_1^2\left[k_{11}p_2^2 + k_{22}p_3^2 + k_{12}p_2p_3 + k_1p_2 + k_2p_3 + k_0\right] =: 4a^2c_1^2g(p_2,p_3).
\end{aligned}$$

To calculate the extremum of $g(p_2, p_3)$,

$$\nabla g(\hat{p}_2, \hat{p}_3) = \begin{pmatrix} 2k_{11}\hat{p}_2 + k_{12}\hat{p}_3 + k_1 \\ k_{12}\hat{p}_2 + 2k_{22}\hat{p}_3 + k_2 \end{pmatrix} = \begin{pmatrix} 0 \\ 0 \end{pmatrix}$$

is necessary, which leads to

$$\hat{p}_2 = \frac{2k_1k_{22} - k_2k_{12}}{k_{12}^2 - 4k_{11}^2k_{22}^2}, \quad \hat{p}_3 = \frac{2k_2k_{11} - k_1k_{12}}{k_{12}^2 - 4k_{11}^2k_{22}^2}, \quad \text{where } k_{12}^2 - 4k_{11}^2k_{22}^2 = q_1q_2q_3$$

with

$$\begin{aligned} q_1 &= {\eta_2}^2{\eta_3}^2, \quad q_2 = -2\,{\xi_1}^2{\xi_2}^2 - 2\,{\xi_1}^2{\xi_3}^2 - 2\,{\xi_2}^2{\xi_3}^2 + {\xi_1}^2 + {\xi_2}^2 + {\xi_3}^2 + 3 \in [0, 4], \\ q_3 &= 8\,{\xi_1}^4{\xi_2}^2{\xi_3}^2 + 4\,{\xi_1}^2{\xi_2}^4{\xi_3}^2 + 4\,{\xi_1}^2{\xi_2}^2{\xi_3}^4 + 4\,{\xi_2}^4{\xi_3}^4 - 4\,{\xi_1}^4{\xi_2}^2 \\ &\quad - 4\,{\xi_1}^4{\xi_3}^2 - 22\,{\xi_1}^2{\xi_2}^2{\xi_3}^2 - 6\,{\xi_2}^4{\xi_3}^2 - 6\,{\xi_2}^2{\xi_3}^4 + 8\,{\xi_1}^2{\xi_2}^2 \\ &\quad + 8\,{\xi_1}^2{\xi_3}^2 + 20\,{\xi_2}^2{\xi_3}^2 - 2\,{\xi_1}^2 - 3\,{\xi_2}^2 - 3\,{\xi_3}^2 - 6 \in [-9, 0]. \end{aligned}$$

It holds that $q_1q_2q_3 \neq 0$ for $(\xi_2^2, \xi_3^2) \neq (1, 1)$. Since this is the unique root of ∇g, as $k_{11}, k_{22} \geq 0$, we have a minimum at $(p_2, p_3) = (\hat{p}_2, \hat{p}_3)$. We obtain $g(\hat{p}_2, \hat{p}_3) = q_4q_5/q_6$, where

$$\begin{aligned} q_4 &= 2\eta_1^2\left(2\xi_1^2\xi_2^2 + 2\xi_1^2\xi_3^2 + 2\xi_2^2\xi_3^2 - \xi_1^2 - \xi_2^2 - \xi_3^2 - 3\right) \leq 2\eta_1^2\left(\xi_1^2 + \xi_2^2 + \xi_3^2 - 3\right) \leq 0, \\ q_5 &= 8\xi_1^4\xi_2^4\xi_3^2 + 8\xi_1^4\xi_2^2\xi_3^4 + 8\xi_1^2\xi_2^4\xi_3^4 - 4\xi_1^4\xi_2^4 - 20\xi_1^4\xi_2^2\xi_3^2 - 4\xi_1^4\xi_3^4 - 20\xi_1^2\xi_2^4\xi_3^2 - 20\xi_1^2\xi_2^2\xi_3^4 \\ &\quad - 4\xi_2^4\xi_3^4 + 6\xi_2^2\xi_1^4 + 6\xi_1^4\xi_3^2 + 6\xi_1^2\xi_2^4 + 57\xi_1^2\xi_2^2\xi_3^2 + 6\xi_1^2\xi_3^4 + 6\xi_2^4\xi_3^2 + 6\xi_2^2\xi_3^4 \\ &\quad - 20\xi_2^2\xi_1^2 - 20\xi_1^2\xi_3^2 - 20\xi_2^2\xi_3^2 + 3\xi_1^2 + 3\xi_2^2 + 3\xi_3^2 + 6 \in [0, 9], \\ q_6 &= 8\xi_1^4\xi_2^2\xi_3^2 + 4\xi_1^2\xi_2^4\xi_3^2 + 4\xi_1^2\xi_2^2\xi_3^4 + 4\xi_2^4\xi_3^4 - 4\xi_2^2\xi_1^4 - 4\xi_1^4\xi_3^2 - 22\xi_1^2\xi_2^2\xi_3^2 \\ &\quad - 6\xi_2^4\xi_3^2 - 6\xi_2^2\xi_3^4 + 8\xi_2^2\xi_1^2 + 8\xi_1^2\xi_3^2 + 20\xi_2^2\xi_3^2 - 2\xi_1^2 - 3\xi_2^2 - 3\xi_3^2 - 6 \in [-9, 0], \end{aligned}$$

with $q_6 \neq 0$ for $(\xi_2^2, \xi_3^2) \neq (1, 1)$. Hence, in all three cases we conclude that $d_{2,2} \geq 0$, and $D_G \geq 0$ holds.

We still need to show that $D_G > 0$ for all $\xi_1, \xi_2, \xi_3 \in [-1, 1]$. It holds that $d_0 > 0$ for all $(\xi_1, \xi_2, \xi_3) \in [-1, 1]^3 \setminus \{-1, 1\}^3$ as $a < 0$ and $k > 0$. This leads to $D_G > 0$ in these cases. For the case $(\xi_1, \xi_2, \xi_3) \in \{-1, 1\}^3$ we have $m_2(\xi_1, \xi_2, \xi_3) = 3$, which leads to $d_{4,0} = 36a^2 > 0$ and $D_G > 0$. Therefore, $D_G > 0$ holds for all $(\xi_1, \xi_2, \xi_3) \in [-1, 1]^3$, and condition (7.1) is satisfied. ∎

For the more general case with nonvanishing cross-derivatives we have the following result. The comments made in the previous section also apply here.

LEMMA 7.4. *For $a_i = a < 0$, $\Delta x_i = h > 0$ for $i = 1, 2, 3$, and arbitrary $b_{1,2}$, $b_{1,3}$, and $b_{2,3}$, the high-order compact scheme* (6.1) *with the coefficients for the three-dimensional case defined in section* 5.2 *satisfies (for frozen coefficients) the stability condition* (7.1) *at the corner points $\xi_1 = \pm 1$, $\xi_2 = \pm 1$, and $\xi_3 = \pm 1$.*

Proof. Using $\sin(z_1/2) = \sqrt{1 - \xi_1^2} = 0$ for $\xi_1 = \pm 1$, $\sin(z_2/2) = \sqrt{1 - \xi_2^2} = 0$ for $\xi_2 = \pm 1$, and $\sin(z_3/2) = \sqrt{1 - \xi_3^2} = 0$ for $\xi_3 = \pm 1$, straightforward computation yields—just as in the two-dimensional spatial setting—$|G|^2 - 1 = 0$ for all corner points. Hence, condition (7.1) is satisfied. ∎

8. Application to Black–Scholes basket options. To illustrate the practicality of the proposed scheme we now consider the n-dimensional Black–Scholes option pricing partial differential equation (see, e.g., [23]). In the option pricing

problem mixed derivatives appear naturally from correlation of the underlying assets. After transformations, the conditions (4.2) are satisfied, and we give the coefficients of the resulting scheme. Then we discuss the boundary conditions as well as the time discretization.

8.1. Transformation of the *n*-dimensional Black–Scholes equation. In the multidimensional Black–Scholes model the asset prices follow a geometric Brownian motion,

$$dS_i(t) = (\mu_i - \delta_i)S_i(t)dt + \sigma_i S_i(t)dW_i(t), \tag{8.1}$$

where S_i is the ith underlying asset which has an expected return of μ_i, a continuous dividend of δ_i, and the volatility σ_i for $i = 1, \dots, n$ and $n \in \mathbb{N}$. The Wiener processes are correlated with $\langle dW_i, dW_j \rangle =: \rho_{i,j}dt$ for $i, j = 1, \dots, n$ with $i \neq j$. Application of Itô's lemma and standard arbitrage arguments show that any option price $V(S, \sigma, t)$ solves the n-dimensional Black–Scholes partial differential equation,

$$\frac{\partial V}{\partial t} + \frac{1}{2}\sum_{i=1}^{n} \sigma_i^2 S_i^2 \frac{\partial^2 V}{\partial S_i^2} + \sum_{\substack{i,j=1 \\ i<j}}^{n} \rho_{ij}\sigma_i\sigma_j S_i S_j \frac{\partial^2 V}{\partial S_i \partial S_j} + \sum_{i=1}^{n} \eta_i S_i \frac{\partial V}{\partial S_i} - rV = 0, \tag{8.2}$$

where $\eta_i = r - \delta_i$. The transformations

$$x_i = \gamma \ln\left(S_i/K\right)/\sigma_i, \quad \tau = T - t, \quad \text{and} \quad u = e^{r\tau}V/K \tag{8.3}$$

for $i = 1, \dots, n$, where γ is a constant scaling parameter to assure that the resulting computational domain does not get too large, lead to

$$u_\tau - \frac{\gamma^2}{2}\sum_{i=1}^{n} \frac{\partial^2 u}{\partial x_i^2} - \gamma^2 \sum_{\substack{i,j=1 \\ i<j}}^{n} \rho_{ij} \frac{\partial^2 u}{\partial x_i \partial x_j} + \gamma \sum_{i=1}^{n} \varsigma_i \frac{\partial u}{\partial x_i} = 0, \tag{8.4}$$

where $\varsigma_i = \sigma_i/2 - \eta_i/\sigma_i$. Comparing this equation with (2.1), we identify

$$a_i = -\frac{\gamma^2}{2}, \quad b_{ij} = -\gamma^2\rho_{ij}, \quad c_i = \gamma\varsigma_i, \quad g = 0 \tag{8.5}$$

for $i, j = 1, \dots, n$ and $i < j$. We find that the transformed partial differential equation (8.4) with these coefficients satisfies the conditions given by (4.2) if $\Delta x_i = h$ for a step size $h > 0$ is used. Hence, we are able to obtain a high-order compact scheme in any spatial dimension $n \in \mathbb{N}$.

We consider a European power put basket option; thus the final condition for (8.2) is given by

$$V(S_1, \dots, S_n, T) = \max\left(K - \sum_{i=1}^{n} \omega_i S_i, 0\right)^p,$$

where p is an integer and the asset weights satisfy $\sum_{i=1}^{n} \omega_i = 1$. Applying the transformations (8.3) leads to the initial condition

$$u(x_1, \dots, x_n, 0) = K^{p-1} \max\left(1 - \sum_{i=1}^{n} \omega_i e^{\frac{\sigma_i x_i}{\gamma}}, 0\right)^p. \tag{8.6}$$

8.2. Semidiscrete two-dimensional Black–Scholes equation. In this section we apply our general two-dimensional semidiscrete scheme (see section 5.1) to the two-dimensional Black–Scholes model. To obtain the semidiscrete scheme (5.1) we have to apply (8.5) with $n = 2$ to the coefficients in section 5.1, which gives

$$\hat{K}_{i_1,i_2} = \frac{\gamma^2(5-2\rho_{12}^2)}{3h^2} + \frac{\varsigma_1^2+\varsigma_2^2}{3}, \quad \hat{K}_{i_1\pm1,i_2} = \frac{\gamma^2\rho_{12}^2}{3h^2} \pm \frac{\gamma\varsigma_1}{3h} \mp \frac{\gamma\varsigma_2\rho_{12}}{3h} - \frac{\varsigma_1^2}{6} - \frac{\gamma^2}{3h^2},$$
$$\hat{K}_{i_1,i_2\pm1} = \frac{\gamma^2\rho_{12}^2}{3h^2} \pm \frac{\gamma\varsigma_2}{3h} \mp \frac{\gamma\varsigma_1\rho_{12}}{3h} - \frac{\varsigma_2^2}{6} - \frac{\gamma^2}{3h^2},$$
$$\hat{K}_{i_1\pm1,i_2-1} = \pm\frac{\varsigma_2\varsigma_1}{12} - \frac{\gamma\varsigma_2}{12h} \pm \frac{\gamma\varsigma_1}{12h} - \frac{\gamma\varsigma_1\rho_{12}}{6h} \pm \frac{\gamma\varsigma_2\rho_{12}}{6h} - \frac{\gamma^2}{12h^2} \pm \frac{\gamma^2\rho_{12}}{4h^2} - \frac{\gamma^2\rho_{12}^2}{6h^2},$$
$$\hat{K}_{i_1\pm1,i_2+1} = \frac{\gamma\varsigma_2}{12h} \mp \frac{\varsigma_2\varsigma_1}{12} \pm \frac{\gamma\varsigma_1}{12h} + \frac{\gamma\rho_{12}\varsigma_1}{6h} \pm \frac{\gamma\varsigma_2\rho_{12}}{6h} - \frac{\gamma^2}{12h^2} \mp \frac{\gamma^2\rho_{12}}{4h^2} - \frac{\gamma^2\rho_{12}^2}{6h^2},$$

where $\hat{K}_{l,m}$ is the coefficient of $U_{l,m}(\tau)$ for $l \in \{i_1-1, i_1, i_1+1\}$ and $m \in \{i_2-1, i_2, i_2+1\}$. The coefficients of $\partial_\tau U_{l,m}(\tau)$ are given by

$$M_{i_1,i_2} = \frac{2}{3}, \qquad M_{i_1+1,i_2\pm1} = M_{i_1-1,i_2\mp1} = \pm\frac{\rho_{12}}{24},$$
$$M_{i_1\pm1,i_2} = \frac{1}{12} \mp \frac{h\varsigma_1}{12\gamma}, \qquad M_{i_1,i_2\pm1} = \frac{1}{12} \mp \frac{h\varsigma_2}{12\gamma}.$$

Additionally, it holds that $\tilde{g}(x,\tau) = 0$. This gives a semidiscrete scheme of the form (5.1), where K_x and M_x are time-independent. As in section 6 we apply Crank–Nicolson-type time discretization and obtain the fully discrete scheme for the spatial interior.

8.3. Semidiscrete three-dimensional Black–Scholes equation. In this section we give the semidiscrete scheme (5.1) for the three-dimensional Black–Scholes basket option. Using (8.5) with $n = 3$ in section 5.1 and the supplementary material, we obtain the coefficients $\hat{K}_{k,l,m}$ of $U_{k,l,m}(\tau)$ for $k \in \{i_1-1, i_1, i_1+1\}$, $l \in \{i_2-1, i_2, i_2+1\}$, and $m \in \{i_3-1, i_3, i_3+1\}$, which are

$$\hat{K}_{i_1,i_2,i_3} = \frac{\varsigma_1^2}{3} + \frac{\varsigma_2^2}{3} + \frac{\varsigma_3^2}{3} - \frac{2\gamma^2\rho_{12}^2}{3h^2} - \frac{2\gamma^2\rho_{13}^2}{3h^2} - \frac{2\gamma^2\rho_{23}^2}{3h^2} + \frac{2\gamma^2}{h^2},$$
$$\hat{K}_{i_1\pm1,i_2,i_3} = \pm\frac{\gamma\varsigma_1}{6h} - \frac{\varsigma_1^2}{6} \mp \frac{\gamma\rho_{12}\varsigma_2}{3h} + \frac{\gamma^2\rho_{12}^2}{3h^2} - \frac{\gamma^2}{6h^2} \mp \frac{\gamma\rho_{13}\varsigma_3}{3h} + \frac{\gamma^2\rho_{13}^2}{3h^2},$$
$$\hat{K}_{i_1,i_2\pm1,i_3} = \pm\frac{\gamma\varsigma_2}{6h} - \frac{\varsigma_2^2}{6} \mp \frac{\gamma\varsigma_1}{3h} + \frac{\gamma^2\rho_{12}^2}{3h^2} - \frac{\gamma^2}{6h^2} \mp \frac{\gamma\rho_{23}\varsigma_3}{3h} + \frac{\gamma^2\rho_{23}^2}{3h^2},$$
$$\hat{K}_{i_1,i_2,i_3\pm1} = \pm\frac{\gamma\varsigma_3}{6h} - \frac{\varsigma_3^2}{6} \mp \frac{\gamma\rho_{13}}{3h} + \frac{\gamma^2\rho_{13}^2}{3h^2} - \frac{\gamma^2}{6h^2} \mp \frac{\gamma\rho_{23}\varsigma_2}{3h} + \frac{\gamma^2\rho_{23}^2}{3h^2},$$
$$\hat{K}_{i_1\pm1,i_2-1,i_3} = -\gamma\frac{\varsigma_2 \mp \varsigma_1}{12h} \pm \frac{\varsigma_1\varsigma_2}{12} - \frac{\gamma^2}{12h^2} - \gamma\rho_{12}\frac{\varsigma_1 \mp \varsigma_2}{6h} - \gamma^2\frac{\rho_{12}^2 \mp \rho_{12} \pm \rho_{13}\rho_{23}}{6h^2},$$
$$\hat{K}_{i_1\pm1,i_2+1,i_3} = \gamma\frac{\varsigma_2 \pm \varsigma_1}{12h} \mp \frac{\varsigma_1\varsigma_2}{12} - \frac{\gamma^2}{12h^2} + \gamma\rho_{12}\frac{\varsigma_1 \pm \varsigma_2}{6h} - \gamma^2\frac{\rho_{12}^2 \pm \rho_{12} \mp \rho_{13}\rho_{23}}{6h^2},$$
$$\hat{K}_{i_1\pm1,i_2,i_3-1} = -\gamma\frac{\varsigma_3 \mp \varsigma_1}{12h} \pm \frac{\varsigma_1\varsigma_3}{12} - \frac{\gamma^2}{12h^2} - \gamma\rho_{13}\frac{\varsigma_1 \mp \varsigma_3}{6h} - \gamma^2\frac{\rho_{13}^2 \mp \rho_{13} \pm \rho_{12}\rho_{23}}{6h^2},$$
$$\hat{K}_{i_1\pm1,i_2,i_3+1} = \gamma\frac{\varsigma_3 \pm \varsigma_1}{12h} \mp \frac{\varsigma_1\varsigma_3}{12} - \frac{\gamma^2}{12h^2} + \gamma\rho_{13}\frac{\varsigma_1 \pm \varsigma_3}{6h} - \gamma^2\frac{\rho_{13}^2 \pm \rho_{13} \mp \rho_{12}\rho_{23}}{6h^2},$$
$$\hat{K}_{i_1,i_2\pm1,i_3-1} = -\gamma\frac{\varsigma_3 \mp \varsigma_2}{12h} \pm \frac{\varsigma_2\varsigma_3}{12} - \frac{\gamma^2}{12h^2} - \gamma\rho_{23}\frac{\varsigma_2 \mp \varsigma_3}{6h} - \gamma^2\frac{\rho_{23}^2 \mp \rho_{23} \pm \rho_{12}\rho_{13}}{6h^2},$$

$$\hat{K}_{i_1,i_2\pm1,i_3+1} = \gamma\frac{\varsigma_3 \pm \varsigma_2}{12h} \mp \frac{\varsigma_2\varsigma_3}{12} - \frac{\gamma^2}{12h^2} + \gamma\rho_{23}\frac{\varsigma_2 \pm \varsigma_3}{6h} - \gamma^2\frac{\rho_{23}^2 \pm \rho_{23} \mp \rho_{12}\rho_{13}}{6h^2},$$
$$\hat{K}_{i_1\pm1,i_2-1,i_3-1} = \pm\gamma\frac{\rho_{23}\varsigma_1 + \rho_{13}\varsigma_2 + \rho_{12}\varsigma_3}{24h} - \gamma^2\frac{\rho_{23} \mp \rho_{12} \mp \rho_{13}}{24h^2} - \gamma^2\frac{\rho_{12}\rho_{13} \mp \rho_{12}\rho_{23} \mp \rho_{13}\rho_{23}}{12h^2},$$
$$\hat{K}_{i_1\pm1,i_2+1,i_3-1} = \mp\gamma\frac{\rho_{23}\varsigma_1 + \rho_{13}\varsigma_2 + \rho_{12}\varsigma_3}{24h} + \gamma^2\frac{\rho_{23} \mp \rho_{12} \pm \rho_{13}}{24h^2} + \gamma^2\frac{\rho_{12}\rho_{13} \pm \rho_{12}\rho_{23} \mp \rho_{13}\rho_{23}}{12h^2},$$
$$\hat{K}_{i_1\pm1,i_2-1,i_3+1} = \mp\gamma\frac{\rho_{23}\varsigma_1 + \rho_{13}\varsigma_2 + \rho_{12}\varsigma_3}{24h} + \gamma^2\frac{\rho_{23} \pm \rho_{12} \mp \rho_{13}}{24h^2} + \gamma^2\frac{\rho_{13}\rho_{23} \mp \rho_{12}\rho_{23} \pm \rho_{12}\rho_{13}}{12h^2},$$
$$\hat{K}_{i_1\pm1,i_2+1,i_3+1} = \pm\gamma\frac{\rho_{23}\varsigma_1 + \rho_{13}\varsigma_2 + \rho_{12}\varsigma_3}{24h} - \gamma^2\frac{\rho_{23} \pm \rho_{12} \pm \rho_{13}}{24h^2} - \gamma^2\frac{\rho_{12}\rho_{23} \pm \rho_{12}\rho_{13} \pm \rho_{13}\rho_{23}}{12h^2}.$$

Similarly, we get the coefficients $\hat{M}_{k,l,m}$ of $\partial_\tau U_{k,l,m}(\tau)$, given by

$$\hat{M}_{i\pm1,j,m-1} = \hat{M}_{i\mp1,j,m+1} = \mp\frac{\rho_{13}}{24}, \qquad \hat{M}_{i,j\pm1,m-1} = \hat{M}_{i,j\mp1,m+1} = \mp\frac{\rho_{23}}{24},$$
$$\hat{M}_{i\pm1,j-1,m} = \hat{M}_{i\mp1,j+1,m} = \mp\frac{\rho_{12}}{24}, \qquad \hat{M}_{i\pm1,j,m} = \frac{1}{12} \mp \frac{h\varsigma_1}{12\gamma},$$
$$\hat{M}_{i,j\pm1,m} = \frac{1}{12} \mp \frac{h\varsigma_2}{12\gamma}, \qquad \hat{M}_{i,j,m\pm1} = \frac{1}{12} \mp \frac{h\varsigma_3}{12\gamma}, \quad \hat{M}_{i,j,m} = \frac{1}{2},$$
$$\hat{M}_{i\pm1,j-1,m+1} = \hat{M}_{i\pm1,j+1,m+1} = 0, \qquad \hat{M}_{i\pm1,j-1,m-1} = \hat{M}_{i\pm1,j+1,m-1} = 0.$$

Additionally, we have $\tilde{g}(x,\tau) = 0$. We obtain a semidiscrete scheme of the form (5.1), where K_x and M_x are time-independent. As in section 6 we apply Crank–Nicolson-type time discretization and obtain the fully discrete scheme for the spatial interior.

8.4. Treatment of the boundary conditions. Having derived a high-order compact scheme for the spatial interior, we now discuss the boundary conditions.

8.4.1. Lower boundaries. The first boundary we discuss is $S_i = 0$ for some $i \in I \subset \{1,\dots,n\}$ at time $t \in [0,T[$. Once the value of the asset is zero, it stays constant over time; see (8.1). Hence, using $S_i = 0$ for $i \in I$ in (8.2) and applying the transformation (8.3) leads to

$$-\frac{\gamma^2}{2}\sum_{\substack{i=1\\ i\notin I}}^{n}\frac{\partial^2 u}{\partial x_i^2} - \gamma^2\sum_{\substack{i,j=1\\ i,j\notin I\\ i<j}}^{n}\rho_{ij}\frac{\partial^2 u}{\partial x_i\partial x_j} + \gamma\sum_{\substack{i=1\\ i\notin I}}^{n}\varsigma_i\frac{\partial u}{\partial x_i} = f,$$

with $f = -u_\tau$. Hence, at these boundaries we are able to obtain high-order compact schemes in the same manner as shown for the spatial interior, but now with $n - |I|$ spatial dimensions, as the coefficients of the partial differential equations of these boundaries satisfy condition (4.2). The case $I = \{1,\dots,n\}$, i.e., $|I| = n$, leads to the Dirichlet boundary condition $u(x_{\min}^{(1)},\dots,x_{\min}^{(n)},\tau) = u(x_{\min}^{(1)},\dots,x_{\min}^{(n)},0)$ at time $\tau \in]0,\tau_{\max}]$, since in that case $u_\tau = 0$.

8.4.2. Upper boundaries. Upper boundaries are boundaries with $S_i = S_i^{\max}$ for some $i \in J \subset \{1,\dots,n\}$ at time $t \in [0,T[$. For a sufficiently large $S_i^{\max}$ for $i \in J$, we set

$$\left.\frac{\partial V(S_1,\dots,S_n,t)}{\partial S_i}\right|_{S_i=S_i^{\max}} \equiv 0,$$

with $S_k \in \left[S_k^{\min}, S_k^{\max}\right]$ for $k = \{1, \ldots, n\} \setminus \{i\}$ for a European power put basket option. Employing this in (8.2) and using the transformations (8.3) yields

$$-\frac{\gamma^2}{2} \sum_{\substack{i=1 \\ i \notin J}}^{n} \frac{\partial^2 u}{\partial x_i^2} - \gamma^2 \sum_{\substack{i,j=1 \\ i,j \notin J \\ i<j}}^{n} \rho_{ij} \frac{\partial^2 u}{\partial x_i \partial x_j} + \gamma \sum_{\substack{i=1 \\ i \notin J}}^{n} \varsigma_i \frac{\partial u}{\partial x_i} = f, \tag{8.7}$$

with $f = -u_\tau$. Hence the upper boundaries show the same behavior as the lower boundaries for a European power put basket option. Analogously, we have the Dirichlet boundary condition $u(x_{\max}^{(1)}, \ldots, x_{\max}^{(n)}, \tau) = u(x_{\max}^{(1)}, \ldots, x_{\max}^{(n)}, 0)$ for $\tau \in]0, \tau_{\max}]$ if $J = \{1, \ldots, n\}$.

8.5. Combination of upper and lower boundaries. A combination of upper and lower boundaries thus behaves in the same manner, and the resulting partial differential equations with $n - |I| - |J|$ spatial dimensions satisfy condition (4.2) as well. For the corner points of Ω we have $|I| + |J| = n$ and thus again $u = u_0$.

9. Numerical experiments for Black–Scholes basket options. In this section we discuss the numerical experiments for the Black–Scholes power put basket options in spatial dimensions $n = 2, 3$. The equation systems which have to be solved over time have been derived in section 8. According to [13], we cannot expect fourth-order convergence if the initial condition is not sufficiently smooth. Hence, we have to smooth the initial condition for power puts with $p = 1, 2$. In [13] suitable smoothing operators are identified in Fourier space. Since the order of convergence of our high-order compact scheme is four, we use the smoothing operator Φ_4, given by its Fourier transform

$$\hat{\Phi}_4(\omega) = \left(\frac{\sin(\omega/2)}{\omega/2}\right)^4 \left[1 + \frac{2}{3}\sin^2(\omega/2)\right].$$

This leads to the smoothed initial condition

$$\tilde{u}_0(x_1, x_2) = \frac{1}{h^2} \int_{-3h}^{3h} \int_{-3h}^{3h} \Phi_4\left(\frac{x}{h}\right) \Phi_4\left(\frac{y}{h}\right) u_0(x_1 - x, x_2 - y)\, \mathrm{d}x\, \mathrm{d}y,$$

in the case $n = 2$ for any step size $h > 0$, where u_0 is the original initial condition and $\Phi_4(x)$ denotes the Fourier inverse of $\hat{\Phi}_4(\omega)$; see [13]. If u_0 is smooth enough in the integrated region around $(x_1, \ldots, x_n)$, we have $\tilde{u}_0(x_1, \ldots, x_n) = u_0(x_1, \ldots, x_n)$. That means that it is possible to identify the points where smoothing is necessary.

Figure 1 shows an example of a two-dimensional grid on the left-hand side, and on the right-hand side it shows a graph of the nondifferentiable points of the initial condition given in (8.6) together with the identified grid points, where smoothing is necessary. The points are chosen in such a way that we ensure that the nondifferentiable points have no influence on $\tilde{u}_0(x_1, x_2)$ for those points, which are not shown in Figure 1 on the right-hand side. This approach reduces the necessary calculations significantly. As $h \to 0$, the smooth initial condition $\tilde{u}_0$ converges toward the original initial condition u_0 given in (8.6). The results in [13] guarantee high-order convergence of the approximation of the smoothed problem to the true solution of (8.4).

We use the relative l^2-error $\|U_{\mathrm{ref}} - U\|_{l^2} / \|U_{\mathrm{ref}}\|_{l^2}$, as well as the l^∞-error $\|U_{\mathrm{ref}} - U\|_{l^\infty}$, to examine the numerical convergence rate, where U_{ref} denotes a reference

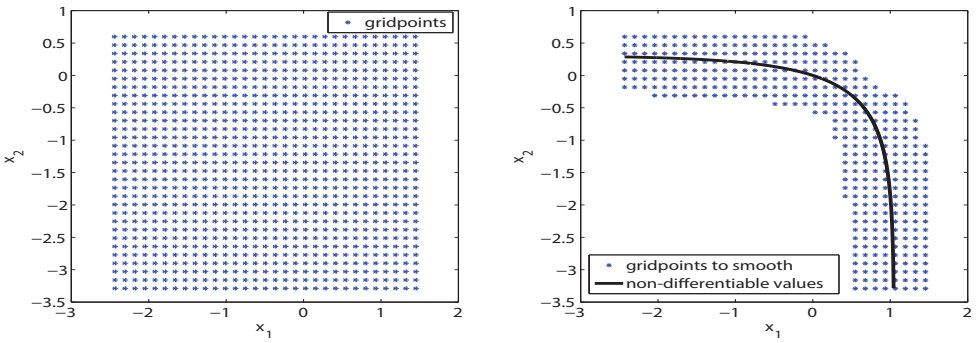

FIG. 1. *Example of grid points selected for the smoothing procedure in two space dimensions. We employ the smoothing operators of Kreiss, Thomee, and Widlund* [13] *to ensure high-order convergence of the approximations of the smoothed problem to the true solution of* (8.4).

solution on a fine grid and U is the approximation. When identifying the convergence order of the schemes, we determine it as the slope of the linear least square fit of the individual error points in the loglog-plots of error versus number of grid points per spatial direction.

9.1. Numerical example with two underlying assets. In this section we report the numerical results for a two-dimensional Black–Scholes power put basket option. We compare the high-order compact scheme ("HOC") with the standard scheme ("2nd order"), which is obtained by using the central difference operator directly in (8.4) for $n = 2$ with no further action and thus leads to a classical second-order scheme. We consider plain European puts ($p = 1$) and use the smoothing procedure outlined above for the initial condition (8.6). The parameter values

$$\sigma_1 = 0.25, \quad \sigma_2 = 0.35, \quad \gamma = 0.25, \quad r = \ln(1.05), \quad \omega_1 = 0.35 = 1 - \omega_2, \quad K = 10,$$

and $\delta_1 = \delta_2 = 0$ are used, unless stated otherwise. The parabolic mesh ratio is fixed to $\Delta\tau/h^2 = 0.4$, although we point out that neither the von Neumann stability analysis nor our numerical experiments revealed any practical restrictions on its choice.

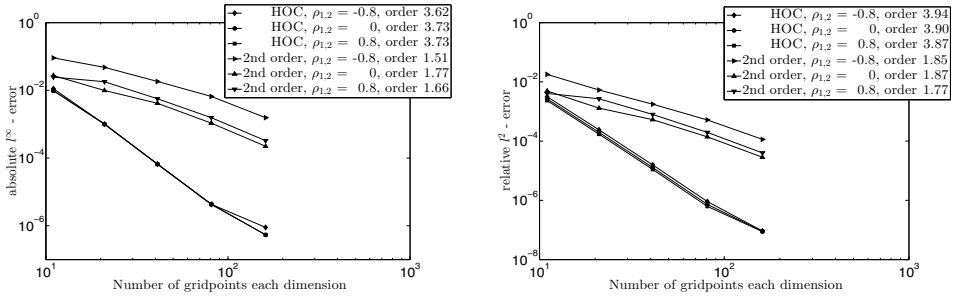

FIG. 2. *l^∞-error (left) and relative l^2-error (right) for two-dimensional Black–Scholes put basket option and smoothed initial condition.*

Figure 2 shows convergence plots for the l^∞-error (left) and for the relative l^2-error (right) for a European put, respectively. The initial condition is smoothed using

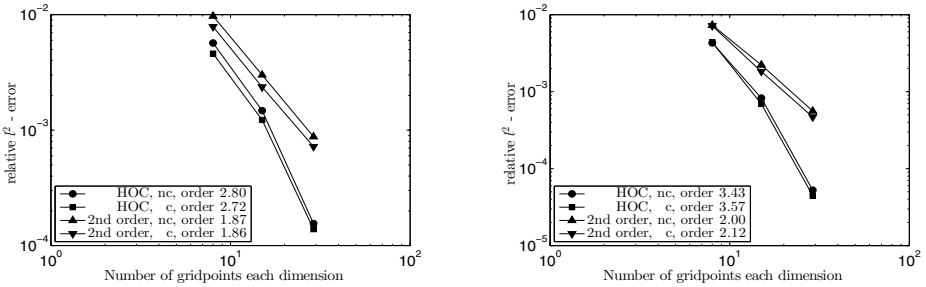

FIG. 3. *Relative l^2-error for three-dimensional Black–Scholes power put basket option, with $p = 3$ (left) and $p = 4$ (right).*

the procedure outlined above. For both types of errors we observe that the numerical convergence rates agree very well with the theoretical orders of the schemes. The high-order compact scheme yields numerical convergence orders close to four and strongly outperforms the standard second-order scheme. The choice of the correlation parameter $\rho_{12} = -0.8$, $\rho_{12} = 0$, and $\rho_{12} = 0.8$ has very little influence.

9.2. Numerical example with three assets. In this section we report on numerical experiments with three underlying assets. We choose the parameters

$$\delta_i = 0.01, \quad \sigma_i = 0.3, \quad \omega_i = 1/3, \quad r = \ln(1.05), \quad \gamma = 0.3, \quad T = 0.25, \quad K = 10.$$

Due to the computational intensity of the three-dimensional problem the number of grid points per spatial dimension is smaller compared to the results in two dimensions reported above. To ensure that at the same time there is a sufficiently large number of grid points in time, we fix the parabolic mesh ratio to $\Delta\tau/h^2 = 0.1$ (not for stability reasons). We perform two types of experiments: without any correlation between the assets (labeled by "nc" in the plots), and with correlation (labeled by "c" in the plots) using the parameter values $\rho_{1,2} = -0.4$, $\rho_{1,3} = -0.1$, $\rho_{2,3} = -0.2$.

We compare the standard approximation to our high-order compact scheme for European power put options with $p = 3, 4$. For the European power puts with $p = 1, 2$, one would smooth the initial condition, as above, to ensure high-order convergence. Figure 3 shows the convergence of the relative l^2-error for a European power put with $p = 3$ and $p = 4$. We use the original initial conditions; no smoothing is applied here. The numerical convergence rates of the high-order compact scheme are slightly reduced to about three and three-and-a-half, respectively. Additional smoothing, which we omitted here to limit the computational load, would result in even better results. Still, the high-order compact scheme outperforms the standard second-order scheme significantly in all cases.

9.3. Numerical example with space-dependent coefficients. In this section we will apply numerical examples for (8.2), where the continuous dividends are dependent on the underlying asset price. For both asset prices S_i with $i = 1, 2$ we consider the following example, where the continuous dividends are zero for small asset prices and then smoothly increase around an asset price $S_i^\star > 0$ toward a given parameter $\delta_i^\star \geq 0$:

$$\delta_i = \delta_i(S_i) = \frac{\delta_i^\star \left[\tanh\left(\zeta_i(S_i - S_i^\star)\right) - \tanh\left(-\zeta_i S_i^\star\right)\right]}{2}.$$

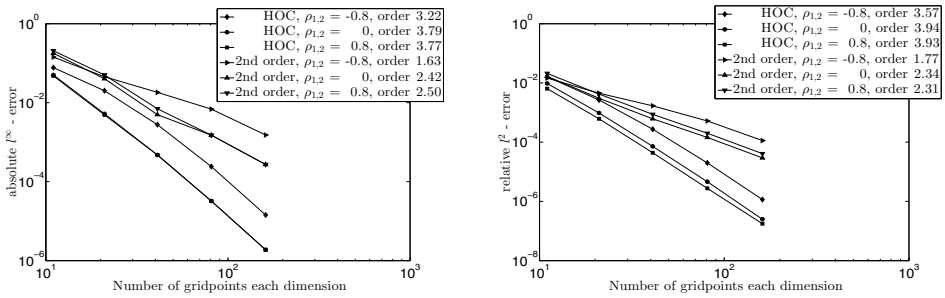

FIG. 4. *l^∞-error (left) and relative l^2-error (right) for two-dimensional Black–Scholes put basket option with space-dependent dividend and smoothed initial condition.*

Financially, the interpretation could be as follows: if the asset is a dividend-paying stock, low stock prices may mean that the company may not be in a financial position to pay dividends. A low value of $\zeta_i > 0$ leads to slow transition from 0 to $\delta_i^\star$. We can apply the transformations given in (8.3) and hence use the coefficients

$$a_i = -\frac{\gamma^2}{2}, \quad b_{ij} = -\gamma^2 \rho_{ij}, \quad c_i = \gamma \left(\frac{\sigma_i}{2} - \frac{r - \delta_i (K e^{\frac{x_i \sigma_i}{\gamma}})}{\sigma_i} \right), \quad g = 0 \tag{9.1}$$

for $i = 1, 2$ to obtain the coefficients of the numerical scheme; see section 5.1. The boundary conditions of section 8.4 are employed, and the parameter values of section 9.1 as well as

$$\delta_1^\star = 0.02, \quad \delta_2^\star = 0.01, \quad \zeta_1 = 0.35, \quad \zeta_2 = 0.5, \quad S_i^\star = 0.9K/\omega_i$$

for $i = 1, 2$ are used in the numerical experiments. Figure 4 shows numerical convergence plots for a European put with space-dependent continuous dividend. Again, smoothing of the initial condition is employed. For the l^∞-error as well as the l^2-error the high-order compact scheme has convergence rates close to four for $\rho_{1,2} = 0$ and $\rho_{1,2} = 0.8$. The convergence rate for the case $\rho_{1,2} = -0.8$ is 3.22 in the l^∞-error, which is mainly due to the two approximations with 11 and 21 grid points per spatial direction, and 3.57 in the l^2-error. The convergence orders of the standard scheme for $\rho_{1,2} = 0, 0.8$ are slightly above two for both types of errors. For $\rho_{1,2} = -0.8$ the convergence orders are noticeably lower as well. In all cases of correlation the high-order compact scheme significantly outperforms the standard second-order scheme.

10. Conclusion. We presented a new high-order compact scheme for a class of parabolic partial differential equations with time- and space-dependent coefficients, including mixed second-order derivative terms in n spatial dimensions. The resulting schemes are fourth-order accurate in space and second-order accurate in time. In a thorough von Neumann stability analysis, where we focused on the case of vanishing mixed derivative terms, we showed that a necessary stability condition holds for frozen coefficients without further conditions in two and three space dimensions. For nonvanishing mixed derivative terms we were able to give partial results. The results suggest unconditional stability of the scheme. As an application example we considered the pricing of European power put basket options in the multidimensional Black–Scholes model. The typical initial conditions of this problem lack sufficient regularity; therefore a suitable smoothing procedure was employed to ensure high-order convergence. In all of the numerical experiments we performed, a comparative standard second-order scheme was significantly outperformed.

Although we derived the scheme in arbitrary space dimension, it was not our aim in this paper to attack the so-called curse of dimensionality. The issue of an exponentially increasing number of unknowns with growing spatial dimension on full grids is, of course, alleviated to some degree by a high-order scheme. To obtain an accuracy similar to that of a second-order scheme which uses $\mathcal{O}(N^d)$ unknowns on a full grid, our high-order compact approach will require "only" $\mathcal{O}(N^{d/2})$ unknowns. To really attack very high-dimensional problems one would need to combine our approach with hierarchical approaches, e.g., using sparse grids (typically requiring $\mathcal{O}(N\ln(N)^{d-1})$ unknowns), which is beyond the scope of the present paper.

Acknowledgment. The authors are grateful to the anonymous reviewers for their constructive comments.

REFERENCES

[1] G. Berikelashvili, M. M. Gupta, and M. Mirianashvili, *Convergence of fourth order compact difference schemes for three-dimensional convection-diffusion equations*, SIAM J. Numer. Anal., 45 (2007), pp. 443–455.

[2] B. Düring and M. Fournié, *High-order compact finite difference scheme for option pricing in stochastic volatility models*, J. Comput. Appl. Math., 236 (2012), pp. 4462–4473.

[3] B. Düring and M. Fournié, *On the stability of a compact finite difference scheme for option pricing*, in Progress in Industrial Mathematics at ECMI 2010, M. Günther et al., eds., Springer-Verlag, Berlin, Heidelberg, 2012, pp. 215–221.

[4] B. Düring, M. Fournié, and C. Heuer, *High-order compact finite difference schemes for option pricing in stochastic volatility models on non-uniform grids*, J. Comput. Appl. Math., 271 (2014), pp. 247–266.

[5] B. Düring, M. Fournié, and A. Jüngel, *High-order compact finite difference schemes for a nonlinear Black-Scholes equation*, Int. J. Theor. Appl. Finance, 6 (2003), pp. 767–789.

[6] B. Düring, M. Fournié, and A. Jüngel, *Convergence of a high-order compact finite difference scheme for a nonlinear Black-Scholes equation*, M2AN Math. Model. Numer. Anal., 38 (2004), pp. 359–369.

[7] M. Fournié and S. Karaa, *Iterative methods and high-order difference schemes for 2D elliptic problems with mixed derivative*, J. Appl. Math. Comput., 22 (2006), pp. 349–363.

[8] M. Fournié and A. Rigal, *High order compact schemes in projection methods for incompressible viscous flows*, Commun. Comput. Phys., 9 (2011), pp. 994–1019.

[9] M. M. Gupta, R. P. Manohar, and J. W. Stephenson, *A single cell high order scheme for the convection-diffusion equation with variable coefficients*, Internat. J. Numer. Methods Fluids, 4 (1984), pp. 641–651.

[10] M. M. Gupta, R. P. Manohar, and J. W. Stephenson, *High-order difference schemes for two-dimensional elliptic equations*, Numer. Methods Partial Differential Equations, 1 (1985), pp. 71–80.

[11] B. Gustafsson, H.-O. Kreiss, and J. Oliger, *Time Dependent Problems and Difference Methods*, John Wiley & Sons, New York, 2013.

[12] S. Karaa and J. Zhang, *Convergence and performance of iterative methods for solving variable coefficient convection-diffusion equation with a fourth-order compact difference scheme*, Comput. Math. Appl., 44 (2002), pp. 457–479.

[13] H. O. Kreiss, V. Thomee, and O. Widlund, *Smoothing of initial data and rates of convergence for parabolic difference equations*, Comm. Pure Appl. Math., 23 (1970), pp. 241–259.

[14] S. K. Lele, *Compact finite difference schemes with spectral-like resolution*, J. Comput. Phys., 103 (1992), pp. 16–42.

[15] M. Li and T. Tang, *A compact fourth-order finite difference scheme for unsteady viscous incompressible flows*, J. Sci. Comput., 16 (2001), pp. 29–45.

[16] M. Li, T. Tang, and B. Fornberg, *A compact fourth-order finite difference scheme for the steady incompressible Navier-Stokes equations*, Internat. J. Numer. Methods Fluids, 20 (1995), pp. 1137–1151.

[17] R. D. Richtmyer and K. W. Morton, *Difference Methods for Initial-Value Problems*, Interscience, New York, 1967.

[18] W. F. Spotz and G. F. Carey, *High-order compact scheme for the steady stream-function vorticity equations*, Internat. J. Numer. Methods Engrg., 38 (1995), pp. 3497–3512.

[19] W. F. Spotz and G. F. Carey, *A high-order compact formulation for the* 3*D Poisson equation*, Numer. Methods Partial Differential Equations, 12 (1996), pp. 235–243.
[20] W. F. Spotz and G. F. Carey, *Extension of high-order compact schemes to time-dependent problems*, Numer. Methods Partial Differential Equations, 17 (2001), pp. 657–672.
[21] J. C. Strickwerda, *Finite Difference Schemes and Partial Differential Equations*, 2nd ed., SIAM, Philadelphia, 2004.
[22] D. Y. Tangman, A. Gopaul, and M. Bhuruth, *Numerical pricing of options using high-order compact finite difference schemes*, J. Comput. Appl. Math., 218 (2008), pp. 270–280.
[23] P. Wilmott, *Derivatives. The Theory and Practice of Financial Engineering*, John Wiley & Sons, Chichester, UK, 1998.